J. Micropalaeontology, 45, 455–474, 2026
https://doi.org/10.5194/jm-45-455-2026

Journal of Micropalaeontology
Open Access

Cuticular microfragments from the lower Cambrian Yanjiahe Formation, China: insights into ecdysozoan biodiversity at the dawn of animal radiation

Lei Zhang[1,2], Fan Zhai[1,2], Ying Wu[1,2], Shan Chang[3], Yan Ye[4,5], Xianguo Lang[1,2], Yanchun Pang[1,2], Liang Hu[1,2], Qinglai Feng[6,7], Marie-Béatrice Forel[8], Taniel Danelian[9], Yuanyuan Yong[10,11], and Jean Vannier[11]

[1]Institute of Sedimentary Geology and State Key Laboratory of Oil and Gas Reservoir Geology and Exploitation & Institute of Sedimentary Geology, Chengdu University of Technology, Chengdu 610059, PR China
[2]Key Laboratory of Deep-time Geography and Environment Reconstruction and Applications of Ministry of Natural Resources, Chengdu University of Technology, Chengdu 610059, PR China
[3]College of Urban and Environmental Sciences, Hubei Normal University, Huangshi 435002, PR China
[4]School of Geosciences, Yangtze University, Wuhan 430100, PR China
[5]Department of Geology, Lund University, Solvegatan 12, 22362 Lund, Sweden
[6]School of Earth Sciences, China University of Geosciences (Wuhan), Wuhan 430074, PR China
[7]State Key Laboratory of Geological Processes and Mineral Resources, China University of Geosciences (Wuhan), Wuhan 430074, PR China
[8]Centre de Recherche en Paléontologie – Paris, UMR7207, MNHN-CNRS-Sorbonne Université, Muséum national d'Histoire naturelle, 8 rue Buffon (CP38), 75005 Paris, France
[9]Univ. Lille, CNRS, UMR 8198 – Evo-Eco-Paleo, 59000 Lille, France
[10]Shaanxi Key Laboratory of Early Life and Environments and State Key Laboratory of Continental Dynamics (SKLCD), Department of Geology, Northwest University, Xi'an 710069, PR China
[11]Université de Lyon, Université Claude Bernard Lyon 1, ENS de Lyon, CNRS, Laboratoire de Géologie de Lyon: Terre, Planètes, Environnement (CNRS-UMR 5276), 69622 Villeurbanne, France

Correspondence: Xianguo Lang (langxianguo19@cdut.edu.cn)

Received: 23 December 2025 – Revised: 5 May 2026 – Accepted: 18 May 2026 – Published: 5 June 2026

Abstract. Ecdysozoa (molting animals) represent one of the most diverse and ecologically successful animal groups in both extant and fossil ecosystems. This study presents new microfossil cuticular evidence from the lower Cambrian (∼ 535 Ma) Yanjiahe Formation (southern China) for ecdysozoan diversity during the Fortunian Stage. Six forms are recognized mainly based on their ornamented cuticular patterns, as well as characters of spines and sclerites, including potentially new scalidophorans and possible fragments of appendage-bearing panarthropods. The fossil assemblage, preserved through phosphatization, includes specimens exceeding 2 mm in size and displays a wide array of cuticular ornamentations organized into three main categories: spiny/sclerite-bearing fragments, appendage-like elements, and other undetermined cuticular remains. Remains of possible appendages (e.g., panarthropods) provide tentative but potentially key insights into the tempo of ecdysozoan radiation. The diversity of cuticular structures suggests the co-occurrence of diverse ecdysozoan body plans during the Fortunian, paralleling the early radiation of other metazoan lineages.

Published by Copernicus Publications on behalf of The Micropalaeontological Society.

1 Introduction

Ecdysozoa (molting animals), including Cycloneuralia and Panarthropoda, represent one of the most diverse and ecologically successful animal groups, both in extant ecosystems and the fossil record (Nielsen, 2012; Brusca et al., 2016; Wang et al., 2023a). Their monophyly is strongly supported by multiple lines of molecular and morphological evidence (Aguinaldo et al., 1997; Giribet and Edgecombe, 2017; Kapli et al., 2021), with molecular clock estimates consistently placing their evolutionary origin in the late Ediacaran Period (Erwin et al., 2011; Rota-Stabelli et al., 2013; Carlisle et al., 2024).

The earliest traces of ecdysozoan activity are recorded in ichnofossils from the terminal Ediacaran to the early Cambrian. A key example from the Ediacaran–Cambrian boundary is *Treptichnus pedum* (Seilacher, 1955; Vannier et al., 2010): it is a complex three-dimensional burrow system widely attributed to vermiform bilaterians, likely priapulid-like worms. Its appearance marks the onset of sustained vertical bioturbation, an ecological shift often termed the "Substrate Revolution" (Bottjer et al., 2000; see also Chen and Liu, 2025). In addition to these burrows, potential evidence for early bilaterian appendages emerges in the upper Ediacaran. Trackways in the Shibantan biota (Three Gorges area, southern China) exhibit locomotion patterns suggestive of paired appendages (Chen et al., 2018b). This interpretation is further supported by younger Terreneuvian trace fossils with morphology more indicative of limb-bearing panarthropods. Notable examples include the resting trace *Rusophycus avalonensis* (Crimes and Anderson, 1985) and the repetitive scratch traces of *Monomorphichnus* and cf. *Allocotichnus dyeri*, both documented from Fortunian phosphorites in southern China, Kazakhstan, and the Newfoundland area, Canada (Zhu, 1997; Weber et al., 2013; Gougeon et al., 2025; Zhang et al., 2025). Nevertheless, the precise identity of the trace-makers, whether panarthropods or other appendage-equipped animals, remains unresolved. A notable temporal gap persists between these early trace fossils and the first unambiguous body fossils of panarthropods, which do not appear until Cambrian Stage 3 (Mángano and Buatois, 2014; Edgecombe, 2020).

Ecdysozoan body fossils from the Ediacaran are rare and controversial (Zhang and Shu, 2021; Howard et al., 2022), although recent studies have proposed potential candidates of the Ecdysozoan body fossil in southern Australia (e.g., *Uncus dzaugisi*; Hughes et al., 2024; Liu, 2025). The lower Cambrian Kuanchuanpu Formation (ca. 535 Ma) has yielded a remarkable diversity of ecdysozoans, dominated by scalidophoran worms preserved in three dimensions via secondary phosphatization, alongside numerous other taxa and undetermined forms (e.g., Liu et al., 2014, 2018; Zhang et al., 2015, 2018; Shao et al., 2020a, b; Zhang, 2022; Qin et al., 2023a, b). This assemblage includes at least nine formally named genera and species, as well as over 10 undescribed forms (Liu et al., 2014, 2018; Zhang et al., 2015, 2018; Shao et al., 2020a, b; Qin et al., 2023a, b). The taxonomic diversity of ecdysozoans in the Kuanchuanpu Formation can be summarized into four main categories: (1) sac-like forms, exemplified by *Saccorhytus coronarius* (Han et al., 2017; Liu et al., 2022); (2) putative kinorhynch-like taxa, including *Eokinorhynchus* and *Zhongpingscolex* (Zhang et al., 2015; Shao et al., 2020a, b); (3) vermiform groups lacking extensive sclerites and spines, represented by *Eopriapulites* (Liu et al., 2018); and (4) vermiform groups exhibiting diverse sclerite and spine morphologies, such as *Xinliscolex*, *Qinscolex*, *Shanscolex*, and *Dahescolex* (Zhang, 2022; Liu et al., 2018; Shao et al., 2020a, b). A notable feature of these assemblages is the absence of panarthropods, except possible lobopodians (Yang et al., 2024). So far, no unambiguous fragmentary cuticular elements or articulated appendages that would reveal the presence of euarthropods have been found before the Cambrian Stage 3 (Edgecombe and Legg, 2014). Nevertheless, these exceptionally preserved fossil assemblages provide unparalleled insights into the early evolutionary history of Ecdysozoa (Edgecombe and Legg, 2014; Chen et al., 2018b, 2019; Wang et al., 2025a, b).

Early scalidophorans exhibit a remarkable diversity of cuticular features – such as scalids, pharyngeal teeth, and trunk sclerites – and grew by molting, as evidenced by well-preserved exuviae (Wang et al., 2019, 2020). *Saccorhytus coronarius*, an iconic member of the Kuanchuanpu fauna initially interpreted as a basal deuterostome (Han et al., 2017), is now confidently placed in the ecdysozoan stem-group (Liu et al., 2022) and may represent the larval stage of a scalidophoran (Vannier, 2024). Recent discoveries of *Beretella spinosa*, exhibiting similar morphology, have led Wang et al. (2024) to suggest a new phylum, Saccorhytida, for these taxa. Recently, Liu et al. (2025) described *Saccus xixiangensis* and *Saccus necopinus* from the lowermost Kuanchuanpu Formation, which show close affinities to *Saccorhytus* and may represent either stem-group or total-group ecdysozoans. Notably, soft tissues and internal organs are rarely preserved in Kuanchuanpu animals. However, Wang et al. (2025b) described the oldest known ventral nerve cord in scalidophorans from this biota, represented by an unpaired linear feature running along the trunk, which has direct equivalence in modern priapulids and nematodes. Fossilized embryos provide additional valuable information on the ontogeny of early ecdysozoans, particularly scalidophorans, with *Markuelia* from the Cambrian Stage 2 (Siberia) being one of the best-studied examples (Dong et al., 2004, 2010; Maas et al., 2006; Haug et al., 2009; Zhang et al., 2011; Steiner et al., 2020).

It is important to note that "Orsten"-type fossils are dominated by micro- and millimetric organisms, some of which may have belonged to meiofauna (Maas et al., 2006). Secondary phosphatization favors the preservation of small organisms, leading to a potential bias in the fossil record, as larger organisms are less likely to be preserved (Zhang et

al., 2018, 2021; Yu et al., 2022). The aim of the present study is to evaluate early ecdysozoan diversity through the analysis of abundant, exceptionally preserved cuticular remains recovered from the lower Yanjiahe Formation in the eastern Three Gorges area (~ 535 Ma). Previous investigations in this region have reported a diverse assemblage of fossils, collectively referred to as the Yanjiahe biota. These include organisms preserved in silty mudstone and small shelly fossils found in intraclastic dolostone (Guo et al., 2009, 2014). Phosphatized microfossils, such as cnidarians and *Beretella spinosa* of the phylum Saccorhytida, have additionally been documented from the upper part of the Yanjiahe Formation (e.g., Guo et al., 2020; Song et al., 2024; Wang et al., 2024). A specimen of *Saccorhytus* has also been identified in the lower part of the formation (Steiner et al., 2020). Despite these findings, the lower Yanjiahe Formation remains relatively underexplored. In this work, we present a substantial collection of "Orsten"-type fossils isolated from the lower Yanjiahe Formation through acetic acid maceration. Although fragmentary, some specimens exceed 2 mm in size and display distinct ornamentation patterns rarely documented in contemporaneous assemblages, such as possible appendages. This new material offers valuable data for refining our understanding of ecdysozoan diversity and provides important clues about their early evolution prior to the main phase of the Cambrian radiation.

2 Geological background

The South China Craton, situated along the northern margin of East Gondwana during the Ediacaran–Cambrian transition (Metcalfe, 2013; Wang et al., 2023b), comprised the Yangtze and Cathaysia blocks separated by the Jiangnan basin (Wang and Li, 2003; Fig. 1A). Its paleogeography featured a complex mosaic of shallow to deep marine environments (Chen et al., 2018a). The Three Gorges area on the northern Yangtze Platform preserves a well-exposed and continuous stratigraphic record of this interval (Guo et al., 2009, 2014). Here, the Huangling anticline contains a complete Ediacaran–Cambrian boundary succession (Steiner et al., 2007; Fig. 1B), beginning with Cryogenian glacial deposits and progressing through Ediacaran carbonates (Chen, 1984). The uppermost Ediacaran Dengying Formation consists of thick dolostones deposited under restricted shallow marine conditions (Zhu et al., 2003, 2007).

A significant lithological shift marks the base of the overlying Yanjiahe Formation (Wang et al., 1998), characterized by mixed carbonate-siliciclastic rocks and chert-dolomite interbeds (Ishikawa et al., 2008; Steiner et al., 2020). At the classic Gunshi'ao section, the Yanjiahe Formation is 54.4 m thick and divided into eight lithologically distinct beds (Fig. 2; Chang et al., 2019), beginning with sandy dolostones and shales (Bed 1) and progressing through intervals dominated by chert-dolomite interbeds (Beds 2–3), phosphatic intraclastic dolostones (Bed 4), and chert-carbonaceous shale alternations (Bed 5), culminating in limestones with siliceous nodules and phosphatic intraclastic limestone (Beds 6–8). The correlative succession at the Muyangxi section is partially covered, exposing only strata equivalent to the uppermost Bed 3 through the lower Bed 5 of the Gunshi'ao section, with the fossiliferous horizons occurring within the intraclastic dolostone unit (Bed 4). At the Gunshi'ao and Muyangxi sections, the lower Yanjiahe Formation contains fossiliferous horizons correlative with the SSF1 small shelly fossil zone and the AHC acritarch assemblage (Guo et al., 2014; Ahn and Zhu, 2017; Chang et al., 2019; Steiner et al., 2020; Zhang et al., 2022, 2025a; Fig. 1C). Radiometric dating constrains the formation to between approximately 540 and 526 million years (Condon et al., 2005; Okada et al., 2014; Lan et al., 2017; Linnemann et al., 2019; Zhang et al., 2022), coinciding with the basal Cambrian carbon isotope excursion and a major faunal turnover marking the rise of Cambrian ecosystems (Zhu et al., 2007; Peng et al., 2012; Wang et al., 2012; Steiner et al., 2020).

3 Materials and methods

Fossil material for this study was obtained from the siliceous-phosphatic dolostone in Bed 4 in the Yanjiahe Formation at the Muyangxi section in the Three Gorges area. Approximately 2000 kg of rock was collected from this horizon for the extraction of three-dimensional small shelly fossils. Laboratory processing was carried out at the Palaeontology Laboratory of Chengdu University of Technology, where samples were subjected to sequential acetic acid (7 %–10 %) digestion over a period of approximately 2 months, with the acid refreshed at regular 72 h intervals. Following complete carbonate dissolution, the residues were wet-sieved through a graded mesh series (10 to 200 mesh), air-dried, and subsequently examined under a binocular microscope for manual specimen recovery. For detailed morphological characterization, selected fossils were sputter-coated with a gold-palladium alloy and analyzed using a field emission scanning electron microscope. Linear dimensions were measured from the least-deformed specimens with the aid of image analysis software (CorelDRAW X7). All illustrated and studied specimens are housed in the collections of the Institute of Sedimentary Geology at Chengdu University of Technology.

4 Results

We present a description of secondarily phosphatized "Orsten"-type fossils recovered from the lower Cambrian (ca. 535 Ma) Yanjiahe Formation exposed at the Muyangxi section in the eastern Three Gorges area, southern China. The collection includes numerous specimens exceeding 2 mm in size, exhibiting complex and well-preserved cuticular microstructures. While many specimens are fragmented, the

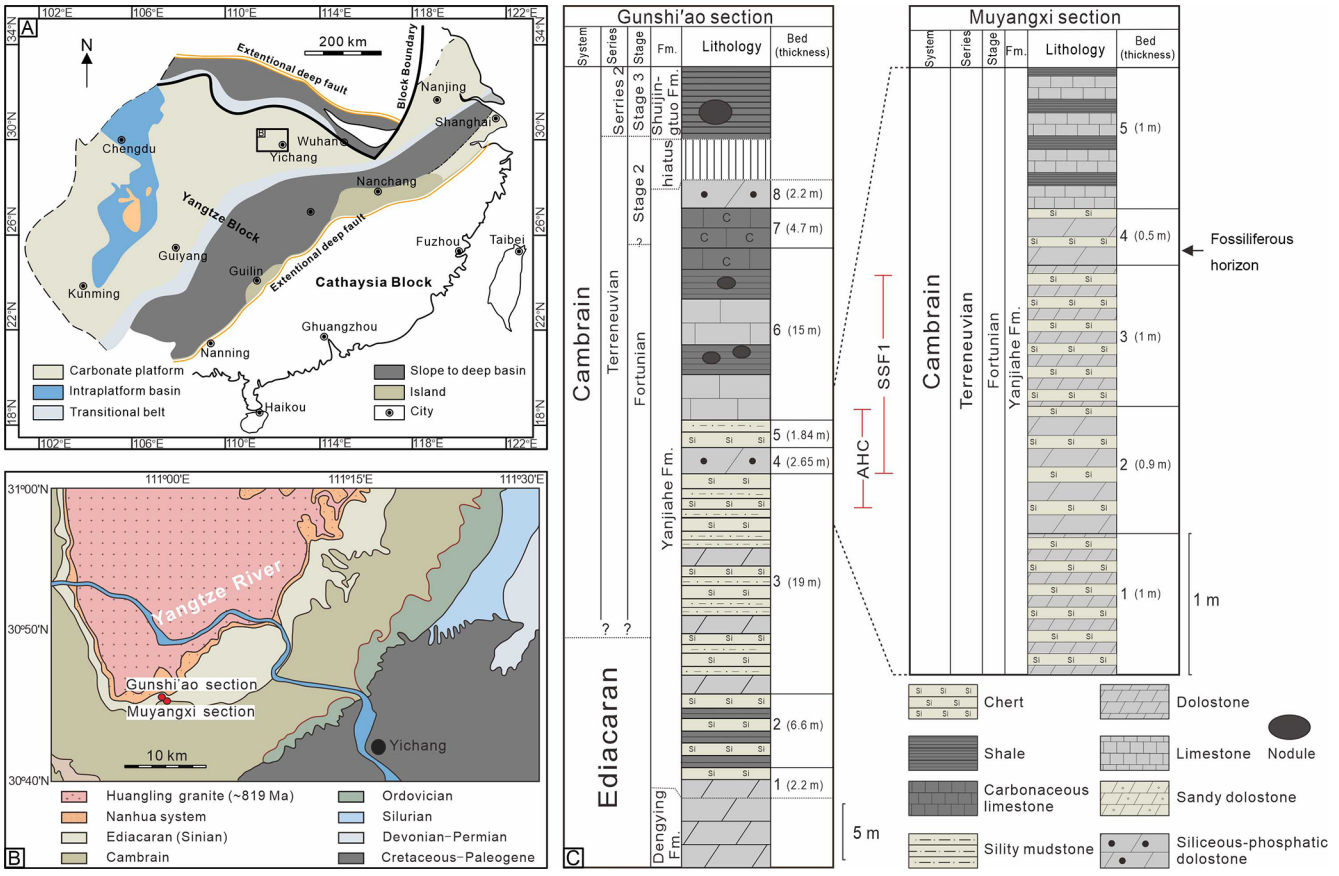

Figure 1. **(A)** Late Ediacaran–early Cambrian paleogeographic reconstruction of the South China Craton (modified after Gao et al., 2021); the black square highlights the study area in the Yangtze Block. **(B)** Geological map of the Three Gorges area (Hubei Province), including the location of the Muyangxi and Gunshi'ao sections (modified after Guo et al., 2009). **(C)** Lithostratigraphy of the Muyangxi and neighboring Gunshi'ao section, including the fossiliferous level studied here and the biozones SSF1 (*Anabarites trisulcatus–Protohertzina anabarica* assemblage zone) and AHC (*Asteridium–Heliosphaeridium–Comasphaeridium* acritarch assemblage zone) (modified after Chang et al., 2019; Zhang et al., 2025a). Fm. = Formation.

high fidelity of preservation enables detailed morphological comparison with established faunas from other localities, such as the Kuanchuanpu biota (Liu et al., 2022). Based primarily on distinct cuticular ornamentation patterns, and spine and sclerite morphology, the studied fossils are categorized into six forms, which are broadly grouped into three morphological categories: cuticular fragments that exhibit appendage-like structures (illustrated in Figs. 2 and 6E, F), cuticular fragments bearing prominent spines or isolated sclerites (Figs. 3, 4, and 5A–C) and other undetermined "cuticular" fragments (illustrated in Figs. 5D–M and 6A–D, G–N). The taxonomic differentiation among these forms is principally founded on the morphology of micro-ornamentation, which includes features such as tubercular protrusions, polygonal reticulation, spines of various shapes, and undulating surface patterns. A simple summary of the key cuticular features across different forms can be found in Table S1 in the Supplement.

5 Morphological description

Measurements are provided in Table S2.

5.1 Cuticular with appendage-like fragments

Form A

Figs. 2 and 6E, F

Materials. Four specimens.

Description. The cuticle displays a vermiform morphology, appearing either C-shaped (Figs. 2A, B, and 6E, F) or cylindrical (Fig. 2C and D) in cross-section depending on preservation state. Two types of ornamentation can be found on these specimens. The first ornamentation consists of broad, sinuous ridges measuring 52–279 µm in width (mean 105.7 µm, $n = 13$), oriented obliquely at approximately 30° (Fig. 2E and F, arrows) to 90° (Fig. 6E and F,

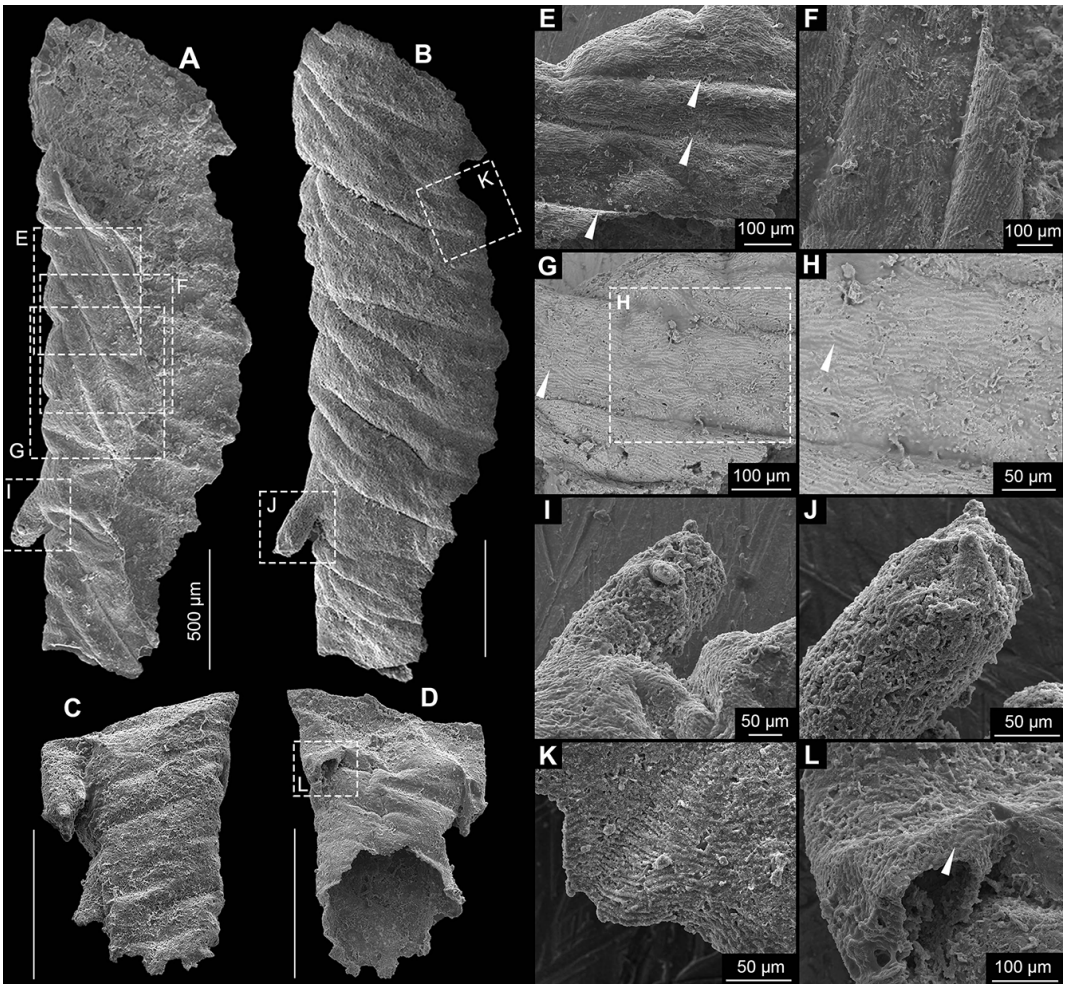

Figure 2. Cuticular Form A. **(A, B)** No. MYX-YJH-1-019. **(C, D)** No. MYX-YJH-1-079. **(E, F)** Detail of Form A in **(A)**, showing the broad, sinuous ridges on the cuticle (arrows), oriented obliquely at approximately 30° to the long axis. **(G)** Detail of Form A in **(A)**, showing finer, more uniform striations on the cuticle. **(H)** Detail of Form A in **(G)**, showing finer, more uniform striations with subtle undulations and bifurcations (arrow). **(I)** Detail of Form A in **(A)**, showing the smaller-diameter tubular branches extending laterally from the main cylindrical body. **(J)** Detail of Form A in **(A)**, showing that finer, more uniform striations can also be found on the branches. **(K,)** Detail of Form B in **(A)**, showing weak polygonal patterns (arrow). Among them, **(G)** and **(H)** are the backscattered electron image, while all the others (including images in all other figures) are secondary electron images. Unlabeled scale bar = 500 µm.

arrows) to the long axis. These ridges show irregular patterns, occasionally bifurcating or merging. The second ornamentation is composed of finer, more uniform striations (Fig. 2G–H and K, arrows) ranging from 4.8 to 6.2 µm in width (mean 5.2 µm, $n = 20$), which generally follow the orientation of the ridges but display subtle undulations, bifurcations (Fig. 2G–H and K, arrows), and localized transitions to weak polygonal patterns (Fig. 2L, arrow) with long axes measuring 4.4–9.8 µm (mean 6.5 µm, $n = 8$). A distinctive feature of Form A is the presence of smaller-diameter tubular branches extending laterally from the main cylindrical body (Fig. 2I and J). The external surface shows minimal taphonomic deformation, with ridge patterns faintly visible on the internal surface while striations remain restricted to the exterior. All of these branches are incompletely preserved, measuring 279 µm in length and 118 µm in width for the specimen in Fig. 2A and B, which has only one branch on the left, and 72 and 132 µm in length and 133 and 116 µm in width for the specimen in Fig. 2C and D, which displays two branches. Form A is notably characterized by the complete absence of spines, tubercles, or sclerites, distinguishing it from most other cuticular types described in this study. Furthermore, some cuticle specimens show no fine striations or branching patterns. Nevertheless, they can be readily attributed to this form based on their distinctive C-shaped contours and broad, undulating ridges, spaced 552–654 µm apart (mean 594.4 µm, $n = 4$), which also run obliquely across the surface of the cuticles. The maximal size of this form is about 3.1 mm (Fig. 7; Table S2).

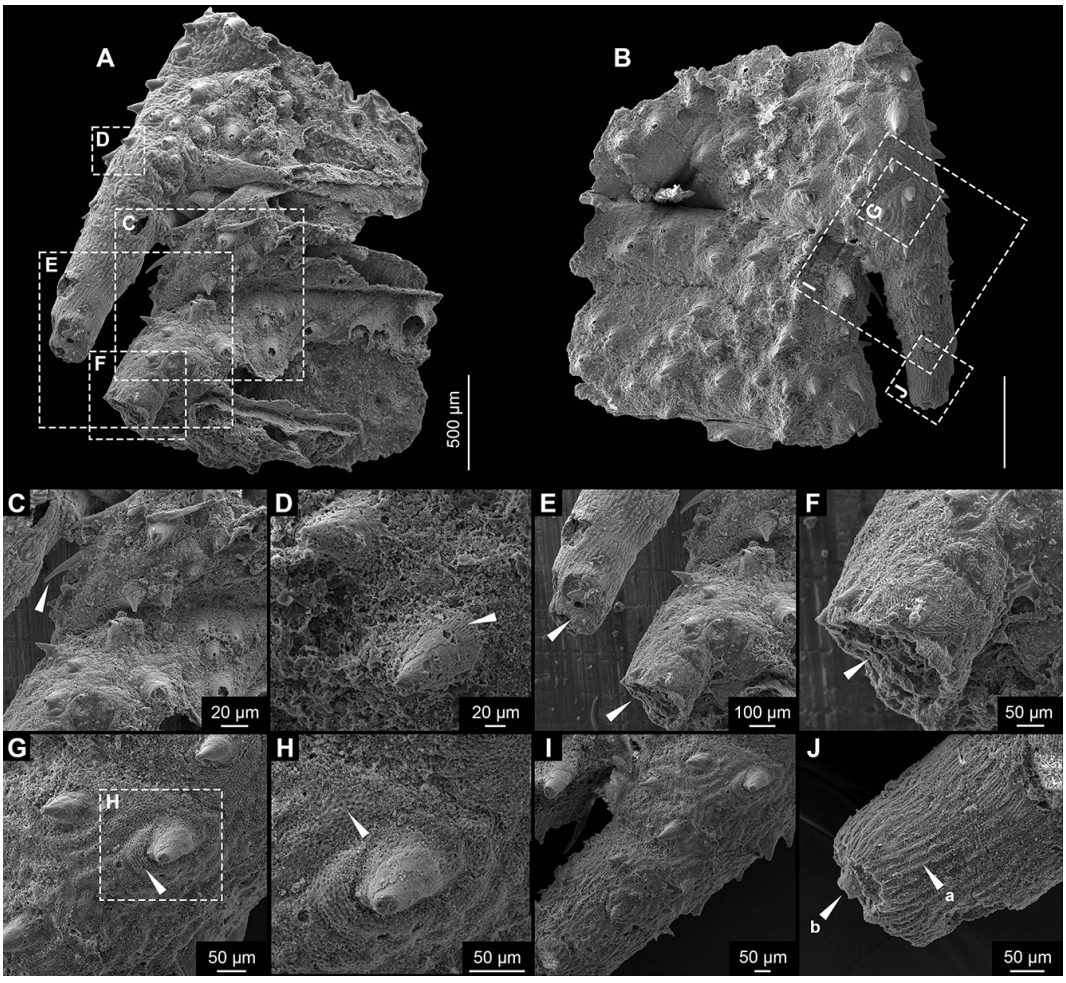

Figure 3. Cuticular Form B. **(A, B)** No. MYX-YJH-1-2407013. **(C, D)** Detail of Form B in **(A)**, showing spines on the trunk and branches. **(E, F)** Detail of Form B in **(A)**, showing tubular, hollow branches extending laterally at ∼ 18° from the trunk. **(G, H)** Detail of Form B in **(B)**, showing closely packed polygonal ornamentation that forms distinct rings around spine bases. **(I, J)** Detail of Form B in **(B)**, showing a proximal-to-distal density gradient of the spines on the branch, with cuticle ornamentation transitioning from polygonal reticulation to fine longitudinal striations; a single terminal spine occurs on the truncate-conical tip. Scale bar (unlabeled) = 500 µm.

Comparisons. While the broad ridges superficially resemble the transverse annulations seen in some worm-like organisms, their oblique orientation (approximately 30° to the long axis) and irregular patterns argue against their interpretation as true annulation or segmentation. Similar ridge patterns have been described in other cuticular fossils (see figs. 3A and 5B in Zhang et al., 2021). The finer striations, however, likely represent primary biological structures. The surface ornamentation, characterized by fine parallel wavy striations, roughly resembles cuticular structures observed in *Yicaris dianensis* (Zhang et al., 2007), the earliest reported crown-group crustacean discovered in the Yu'anshan Formation (Cambrian Series 2, Stage 3) of Yunnan, China, although its drop-shaped pores (Zhang et al., 2007, 2021) are absent in our specimens. Comparable micro-ornamentation also occurs in cnidarian periderms and some earliest ecdysozoan cuticles, including the W-shaped striae on the cuticle of *Saccorhytus*. The localized development of the polygonal pattern in our specimens may tentatively support an ecdysozoan affinity, although this interpretation requires further evidence. The laterally positioned tubular structures resemble appendages of some panarthropods (see Zhang et al., 2007). More detailed discussion can be found in Sect. 6.2.

Occurrence. Lower part of the Yanjiahe Formation, Muyangxi section, eastern Three Gorges area, Cambrian Fortunian.

Form B

Fig. 3

Materials. One specimen.

Description. This fragmented specimen represents a compressed trunk segment, with its original three-dimensional

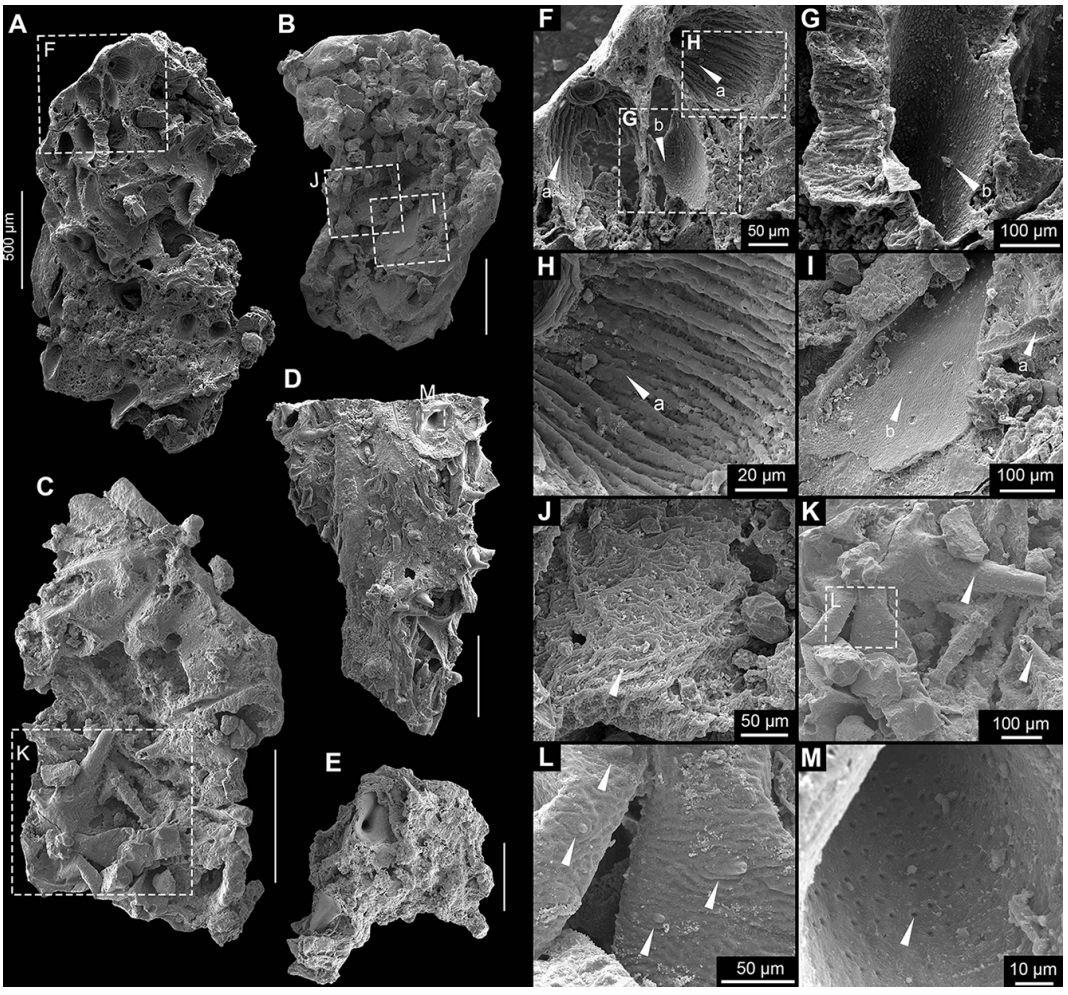

Figure 4. Cuticular Form C. **(A)** No. MYX-YJH-1-083; **(B)** no. MYX-YJH-1-039; **(C)** no. MYX-YJH-1-054; **(D)** no. MYX-YJH-1-074; **(E)** no. MYX-YJH-1-25095. **(F)** Detail of Form C in **(A)**, displaying larger elements comprising tubular spines with dome-shaped bases (arrow a) and coniform spines featuring depressed funnel-shaped bases (arrow b) on the molded counterparts of the cuticle. **(G)** Detail of Form C in **(F)**, also showing larger elements that comprise tubular spines with dome-shaped bases (arrow a) and coniform spines featuring depressed funnel-shaped bases (arrow b) on the molded counterparts of the cuticle. **(H)** Detail of Form C in **(F)**, showing pliable longitudinal striations that may extend into the dome-shaped bases (arrow a) of the spines. **(I)** Detail of Form C in **(B)**, showing the tubular shape of the larger spines (arrow a) and the depressed funnel-shaped bases of the coniform spines (arrow b). **(J)** Detail of Form C in **(B)**, showing interspinal cuticular regions appearing exceptionally flexible, displaying a hierarchical reticulated pattern that consists of smaller irregular ridge-defined polygons superimposed by larger orbit-like meshes. **(K)** Detail of Form C in **(C)**, showing larger coniform spines (arrows) on the cuticle. **(L)** Detail of Form C in **(K)**, showing smaller irregular ridge-defined polygons and smaller coniform spines (arrows) found on the cuticle. **(M)** Detail of Form C in **(D)**, showing relatively regularly distributed perforations on the inner side of some coniform spines (arrow). Unlabeled scale bar = 500 µm.

morphology significantly altered during preservation (Fig. 3A and B). Notably, however, the internal body cavity maintains sufficient structural integrity to allow clear observation (Fig. 3A). Segmentation of the trunk is evident, allowing for the identification of three individual annuli or zonites (Fig. 3A and B). The segments are subequal in length (ca. 1.13 mm). Pronounced constrictions occur at the segment boundaries, affecting both the external and internal morphology (Fig. 3A and B). The specimen exhibits a uniform morphology across its circumference, with no discernible differentiation between dorsal and ventral sides (Fig. 3A and B). Dense ornamentation of spines, ranging in length from approximately 100 to 190 µm (mean 138 µm, $n = 12$), adorns the trunk surface. The spines are conical to blade-like in shape, with their apices curved slightly outward. Furthermore, they exhibit a weak preferential orientation along the trunk's longitudinal axis, possibly aligned toward the inferred posterior direction (Fig. 3C–I, arrows). Spine morphology is consistent across both sides of the fossil, with no discernible difference in form. The

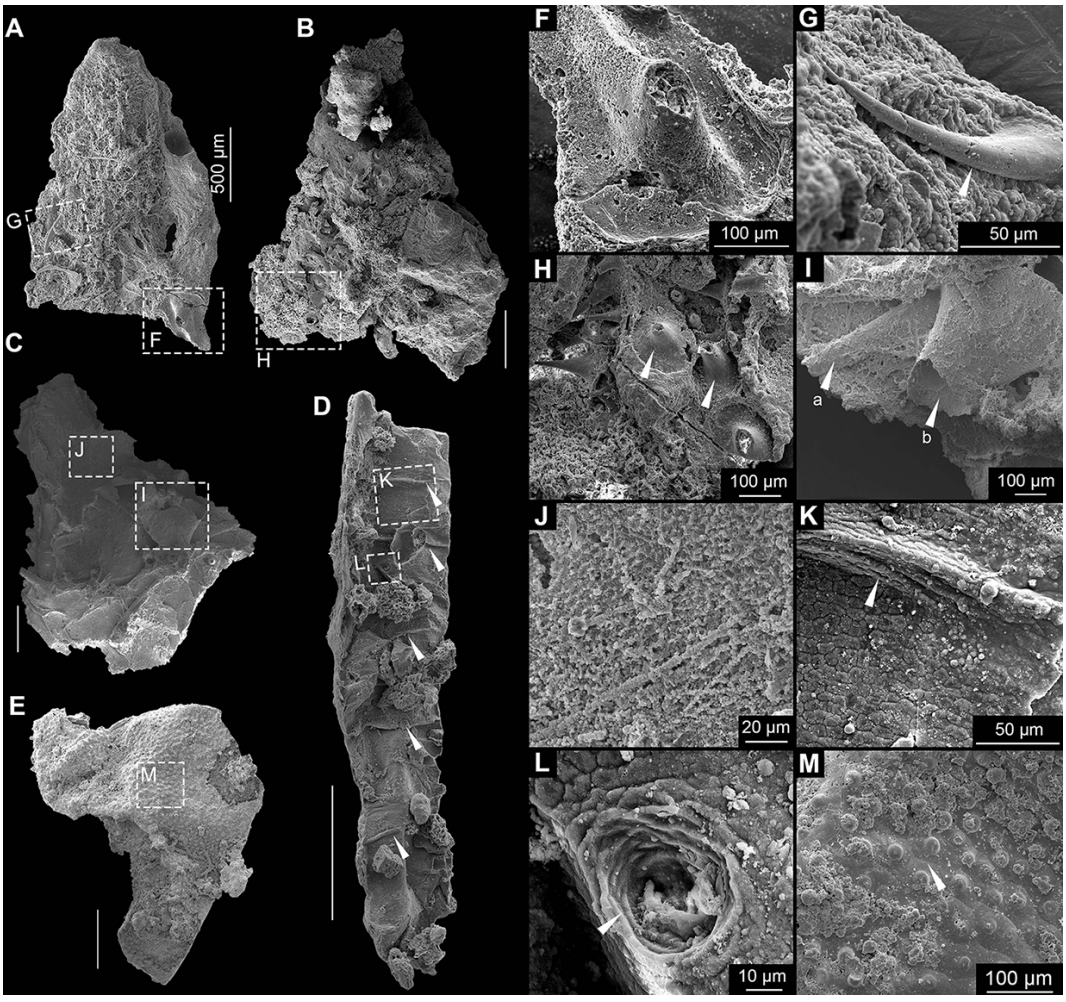

Figure 5. Cuticular forms C–E. **(A–C)** Form C, A, no. MYX-YJH-1-115; **(B)** no. MYX-YJH-1-303; **(C)** no. MYX-YJH-1-187; **(D)** Form D, no. MYX-YJH-1-25196. **(E)** Subtype 1 of Form E, no. MYX-YJH-1-068. **(F)** Detail of Form C in **(A)**, showing a "cowboy hat"-shaped base of the smaller hook-like spines. **(G)** Detail of Form C in **(A)**, showing the smaller hook-like spine (arrow). **(H)** Detail of Form C in **(B)**, showing discoid basal expansions of the smaller coniform spines (arrows). **(I)** Detail of Form C in **(C)**, showing coniform spines with the depressed funnel-shaped bases (arrows). **(J)** Detail of Form C in **(C)**, showing more regular polygonal structures on the cuticle of some foliated specimens. **(K)** Detail of Form C in **(D)**, showing small polygonal ornamentations and a ridge-like bulge (arrow) on the cuticle. **(L)** Detail of Form C in **(D)**, showing small polygonal ornamentations (arrow a) and circular pores or pits (arrow b) on the cuticle. **(M)** Detail of subtype 1 of Form E in **(E)**, showing relatively uniformly distributed papillate knobs on the cuticles. Each knob consists of a hemispherical apex and a broad base, with adjacent papillate knobs separated by pentagonal or hexagonal boundaries (arrow in **M**). Unlabeled scale bar = 500 µm.

cuticle exhibits a well-defined sculpturing of closely packed polygonal units. The maximal size of the polygonal ornaments is about 3.6 to 5.4 µm (mean 4.7 µm, $n = 17$). Each polygon features a central concavity encircled by a faintly elevated rim, with adjacent units sharing these raised margins (Fig. 3G and H). The polygonal ornamentation of the cuticle is particularly well defined around the spine bases, creating a consistent ring that demarcates their points of attachment (Fig. 3G and H, arrows).

The specimen is characterized by lateral branch-like structures (Fig. 3A, B, E, F, I, and J). Although preserved on only one side, their morphology suggests an original bilateral symmetry. Each branch originates from the presumed posterior margin of its segment. The most completely preserved branch is about 1 mm in length, extends laterally at approximately 18° to the trunk axis, and appears oriented posteriorly. This orientation is consistent with the general alignment of the trunk spines (Fig. 3A, B). The branch is tubular, hollow, and circular in cross-section. It tapers distally from a broader proximal region near the trunk (Fig. 3E, F, I, and J, arrows). The incompletely preserved distal extremity suggests a truncate-conical termination, which may have borne

at least one terminal spine, now represented only by its basal remnant (Fig. 3J, arrow). An examination reveals no apparent dorsoventral asymmetry on the branch as well. A second branch on the same side is preserved only at its base; its orientation appears consistent with the more complete branch (Fig. 3E and F, arrows). Spines on the branch match those of the trunk in morphology; however, their distribution shows a pronounced proximal-to-distal gradient, with density gradually declining until they are absent near the tip (Fig. 3I and J). In addition to the spines, the branch cuticle shows a corresponding change in ornamentation. Proximally, it displays polygonal reticulation, which transitions distally into fine, closely spaced longitudinal striations that extend almost to the tip (Fig. 3J). The size of this form is about 2.7 mm (Fig. 7; Table S2).

Comparisons. Form A and Form B are morphologically distinct beyond their shared feature of symmetrical lateral branches. Form B displays clear, well-defined segmentation with boundaries perpendicular to the longitudinal axis, while segmentation in Form A is ambiguous and any divisions are irregularly oriented. The trunk surfaces differ fundamentally. Form A entirely lacks spines and shows a pattern of bifurcating ridges, whereas Form B is densely spinose with a polygonal reticulate ornament. Furthermore, the branches of Form B are more robust and bear longitudinal striations, a transition not seen in Form A. The tubular and lateral nature of these structures suggests a potential comparison to the lobopodous limbs of early panarthropods (Lerosey-Aubril and Ortega-Hernández, 2022; Yang et al., 2024). This interpretation is based on a shared, simplified tubular construction seen in fossils like phosphatized lobopodians (Maas et al., 2007). The comparison, however, is not straightforward. Unlike typical lobopods, these structures lack diagnostic features such as transverse annulations, constrictions, or any form of internal subdivision. Interpreting these structures as annelid parapodia is unlikely because they lack the flattening or lobation typical of such appendages. A comparison to the setae of palaeoscolecids is also difficult, as our specimen is both more robust and lacks the defining annular rings of that group (Xian et al., 2024a). The segmentation and lateral branches of Form B invite comparison with extant kinorhynchs, where the trunk segments could be analogous to zonites and the branches to spines. If valid, this interpretation would suggest the specimen is phylogenetically closer to the kinorhynch crown-group than stem taxa like *Eokinorhynchus rarus* (Zhang et al., 2015). However, key differences challenge this view, as the branches are more robust and integrated, resembling flexible body extensions rather than simple spines. Given these unresolved questions, determining its precise taxonomic placement and evolutionary role will require additional fossil evidence.

Occurrence. Lower part of the Yanjiahe Formation, Muyangxi section, eastern Three Gorges area, Cambrian Fortunian.

5.2 Cuticular fragments with spines and sclerites

Form C

Figs. 4 and 5A–C, F–J

Material. Seventeen specimens.

Description. This is the most abundant form in our materials (Fig. 8). These fragments also display two distinct preservation modes: molded counterparts showing inverted topographical relationships (Fig. 4A and B) and secondary permineralized specimens retaining original surface relief (Fig. 5C). At least four morphologically distinct spine types can be recognized on the relatively large cuticular fragments. The majority of spines are fractured, making it difficult to obtain accurate measurements of their key morphological parameters. Larger elements comprise tubular spines (likely longer than 397.6 µm in height, $n = 6$) with dome-shaped bases (not less than 164.8 µm in maximal width, $n = 2$; Fig. 4A–C and F–H, arrows a; Fig. 4K, arrows) and coniform spines (likely longer than 221.2 µm in height, $n = 4$) featuring depressed funnel-shaped bases (not less than 197.5 µm in maximal width, $n = 3$; Fig. 4A, B, and F–I, arrow b; Fig. 5I, arrows). Smaller elements include coniform spines (not less than 111.2 µm in height, $n = 7$) with flared trumpet-shaped bases (not less than 179.1 µm in maximal width, $n = 7$; Fig. 4D, E, and M, arrow) and blade- or hook-like spines (not less than 326.3 µm in height, $n = 2$, Fig. 5A and G, arrow) exhibiting characteristic "cowboy hat" (Fig. 5A and F) or discoid basal expansions (not less than 471 µm in maximal width, $n = 1$; Fig. 5B and H). All spines are hollow (Fig. 4F–I and M). Relatively regularly distributed perforations can be observed on the inner side of some coniform spines (Fig. 4M, arrow). Their spatial distribution shows no discernible pattern at this stage. In molded specimens, continuous polygonal ornamentation (2.4–9.7 µm in maximal width, mean 5.3 µm, $n = 173$) extending from spine shafts to funnel bases can be found on the inner side of the spines (Fig. 4F, G, and I, arrows b). Generally, the morphological characteristics and maximum of width of the polygons vary across different regions, ranging from 4.45 to 7.54 µm (Fig. 4F, G, and I, arrows b). The transitional zones between spines and cuticle exhibit plicated longitudinal striations (inter-striation spacing: 3.5–8.7 µm, mean 5.3 µm, $n = 18$) that display pronounced folding deformation (Fig. 5F–H). However, this feature could also relate to deformation caused by a change in the angle of the spine during the preservation process, which pulled the cuticle, as not all spine bases exhibit similar plicated structures at their connection points with the cuticles. Dome-shaped bases display relatively less distortion compared to their funnel-shaped counterparts (Fig. 5H, arrows). Interspinal cuticular regions appear exceptionally flexible, displaying a hierarchical reticulated pattern consisting of smaller irregular ridge-defined polygons (between 3.6 and 19.7 µm in maximal width, mean 9.7 µm, $n = 32$) super-

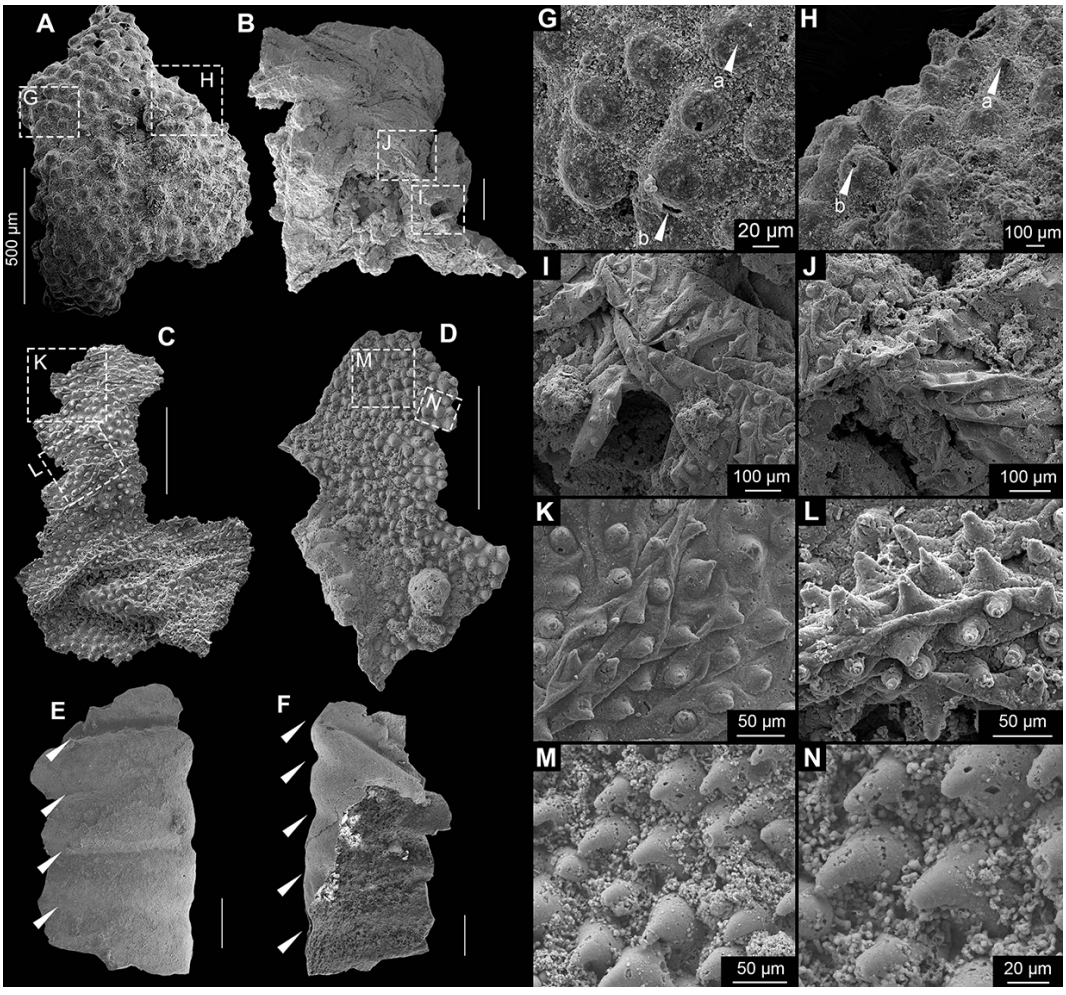

Figure 6. Cuticular forms A, E, and F. **(A)** Subtype 2 of Form E, no. MYX-YJH-1-234. **(B)** Subtype 1 of Form F, no. MYX-YJH-1-24137. **(C)** Subtype 1 of Form F, no. MYX-YJH-1-25010. **(D)** Subtype 2 of Form F, no. MYX-YJH-1-25085. **(E, F)** Form A, no. MYX-YJH-1-25444. **(G)** Detail of subtype 2 of Form F in **A)**, showing the relatively uniformly distributed papillate knob structures but lacking broad bases and polygonal boundaries. Note that the papillate knobs of Form E (subtype 2) should be a thin and hollow exhibit from the broken part (arrow). **(H)** Detail of subtype 2 of Form E in **(A)**, showing the relatively uniformly distributed papillate knob structures but lacking broad bases and polygonal boundaries. The apices of the papillate knob exhibit irregular morphologies, with some specimens tapering into pointed spines (**H**, arrow a) while others develop shallow depressions (**H**, arrow b). **(I, J)** Detail of Form F (subtype 1) in **(B)**, showing densely and uniformly distributed short coniform spines, as well as the twisted and folded features of the cuticle. **(K, L)** Detail of Form F (subtype 1) in **(C)**, also showing densely and uniformly distributed short coniform spines, as well as the twisted and folded features of the cuticle. **(M, N)** Details of Form F (subtype 2) in **(D)**, showing the hook-like spines of the cuticle. Note that the tip of the spines is blunt and rounded. Unlabeled scale bar = 500 µm.

imposed with larger orbit-like meshes (25–40 µm in maximal width, mean 30.2 µm, $n = 29$; Fig. 4J and L). One particularly instructive inverted specimen shows circular depressions at the center of each orbit-like structure, likely representing attachment points for the smaller coniform spines (Fig. 4L, arrows). More regular polygonal structures (Fig. 5J and K) occur on the cuticle of some foliated specimens (Fig. 5C and J). The maximum of size of this form is about 4.3 mm (Fig. 7; Table S2).

Comparisons. The polygonal ornamentation suggests possible ecdysozoan affinities (Mussini and Butterfield, 2025), with particular morphological parallels worth noting. The larger-sized, blade-like spines resemble some SSFs such as the *Protohertzina unguliformis* and *Mongolodus longispinus*, and chaetognath grasping spines (Vannier et al., 2007). The smaller-sized, blade- or hook-like spines with distinctive basal expansions are conversely reminiscent of hooks found on the introvert or trunk of putative Cambrian stem-group scalidophorans and kinorhynchs from the early Cambrian (e.g., *Eokinorhynchus rarus*; Zhang et al., 2015; Shao

et al., 2020a, b) and on the introvert of fossil and living priapulids (Mussini and Butterfield, 2025). In particular, large conical sclerites associated with polygonal cuticular patterns are known in *Scalidodendron* (SCFs, e.g., *Scalidodendron crypticum*; Mussini and Butterfield, 2025). Comparable falcate, hook-like sclerites were likewise present in Cambrian palaeoscolecids, located either on the introvert or trunk (Mussini and Butterfield, 2025). The dome-shaped bases of some coniform spines bear striking similarity to the basal structures of *Saccorhytus*-type protrusions (e.g., the large spine sclerites on the body of *Saccorhytus coronarius*; see Han et al., 2017, and Liu et al., 2022).

Occurrence. Lower part of the Yanjiahe Formation, Muyangxi section, eastern Three Gorges area, Cambrian Fortunian.

5.3 Other fragments

Form D

Figs. 4 and 5A–C

Materials. Two specimens.

Description. These fragments are preserved in their molds; their replica casts reveal that Form D is defined by parallel ridge-like bulges spaced 133–217 µm apart (mean = 172.6 µm, $n = 5$), creating at least six distinct regions (Fig. 5D, arrows; Fig. 5K, arrow). Its surface ornamentation consists of a polygonal reticulation of 7–15 µm (mean = 11.2 µm, $n = 51$; Fig. 4L) units and is further marked by numerous depressed pores, some displaying concentric marginal rings (Fig. 4L, arrows). The largest specimen measures about 1.8 mm across (Fig. 7; Table S2).

Comparisons. The cuticular morphology suggests a possible affinity with vermiform ecdysozoans. The regularly spaced transverse ridges likely represent trunk annulations, while the pores or pits may correspond to the setae of some ecdysozoans (e.g., Xian et al., 2024a). Although contemporaneous Scalidophora fossils also display fine annulations (e.g., *Eopriapulites sphinx*; Liu et al., 2014), the broader annulations here may instead represent macroannuli. This pattern aligns more closely with certain palaeoscolecids, such as *Paleoscolex*, which possess both prominent annulations and setal structures (Xian et al., 2024a). However, the present specimens lack the characteristic sclerites or spines of most palaeoscolecids, which precludes a definitive assignment.

Occurrence. Lower part of the Yanjiahe Formation, Muyangxi section, eastern Three Gorges area, Cambrian Fortunian.

Form E

Figs. 5E, M and 6A, G, H

Materials. Two specimens.

Description. These cuticular fragments are characterized by relatively uniformly distributed papillate knobs (Figs. 5E, 5M and 6A, G, and H). Two subtypes can be recognized in our material. In subtype 1, each knob consists of a hemispherical apex and a broad base, with adjacent papillate knob separated by pentagonal or hexagonal boundaries (Fig. 5E and M). Polygonal fields are irregular and defined by thin grooves (Fig. 5M, arrow). The papillate knobs measure 21–32 µm in diameter (mean 25.2 µm, $n = 30$) with spacings of 30–65 µm (mean 44.9 µm, $n = 49$). The subtype displays comparable papillate knob structures but differs from subtype 1 in several aspects (Fig. 6A, G, and H). First, the papillate knobs are larger, measuring 38–60 µm in diameter (mean 45 µm, $n = 45$) and more closely spaced at 51–107 µm intervals (mean 69.7 µm, $n = 47$). Second, subtype 2 lacks broad bases and polygonal boundaries (Fig. 6A). Third, the broken papillate knobs of subtype 2 exhibit a thin and hollow structure (Fig. 6G, arrow b), which seems to be absent in the apparently solid papillate knobs of subtype 1. Lastly, the apices of the papillate knobs of subtype 2 exhibit irregular morphologies, some of them tapering into pointed spines (Fig. 6H, arrow a), while others develop shallow depressions (Fig. 6G, arrow a; Fig. 6H, arrow b). Both subtypes lack additional cuticular features, and their minimal soft deformation suggests originally thick, rigid textures. The maximal size of this form is about 4.9 mm (Fig. 7; Table S2).

Comparisons. Various papillate knob-bearing fossils have been reported from the Ediacaran to Cambrian, including acanthomorphic acritarchs (e.g., *Bacatisphaera baokangensis* in Zhou et al., 2001; and *Megasphaera cymbala* in Xiao et al., 2014), putative embryos (e.g., *Archaeooides granulatus* in Qian, 1977; and *Archaeooides* sp. in Pyle et al., 2006), algae-like forms (e.g., *Shaanisphaera* in Xian et al., 2024b; and *Qinlingisphaera* in Xian et al., 2024b), and tentative sponges (e.g., *Aetholicopalla* in Luzhnaya et al., 2023). These typically exhibit spherical morphologies with diverse nodules, although some superficial similarities (e.g., depressions on the nodules; see fig. 6G in Xian et al., 2024b) may reflect taphonomic artifacts. Among them, *Megasphaera cymbala* (Xiao et al., 2014) strongly resembles subtype 1 as both are characterized by polygonal sculpture with papillate knobs. However, all the above-mentioned taxa are markedly smaller (generally < 1 mm) than the studied fragments (1.17–2.51 mm in axis length). Similar cones and polygonal patterns also occur on arthropod cuticles or compound eyes in fossil specimens from Cambrian Stage 3 or younger deposits (e.g., Zhang, 1987; Paterson et al., 2011; Lee et al., 2011; Zhang et al., 2021). This cuticular structure also shows some resemblance to putative mollusks

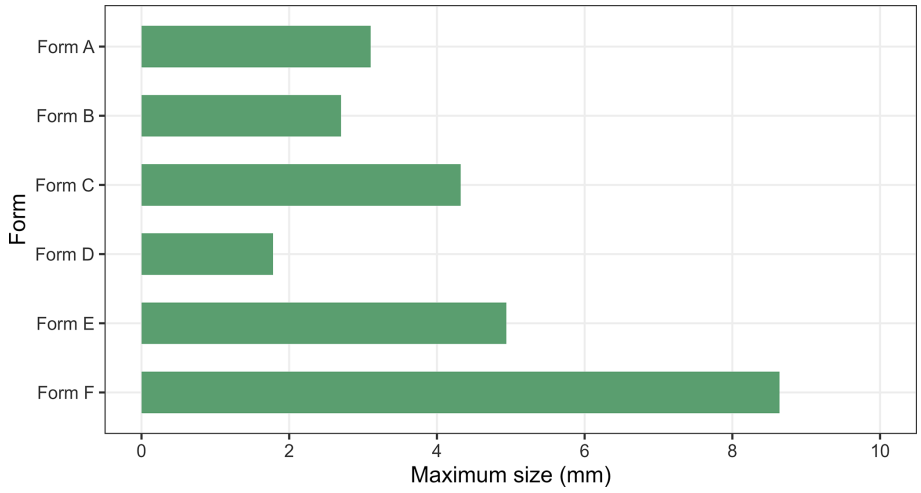

Figure 7. Maximum of size of fragments assigned to each individual fossil form. Detailed data are provided in Table S1.

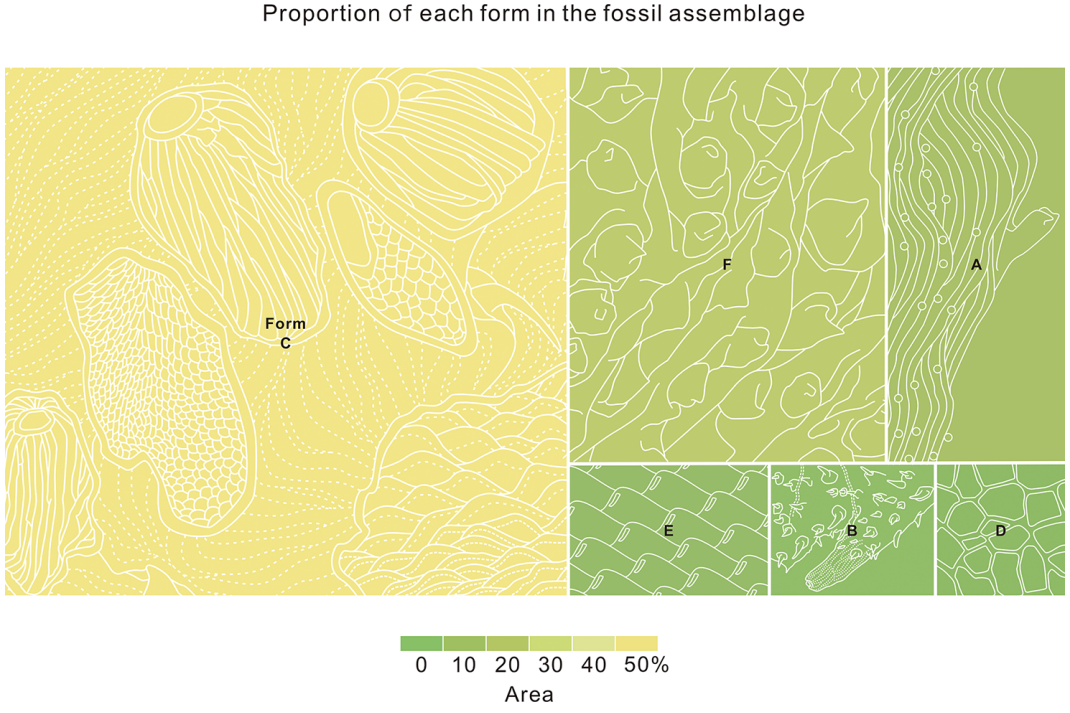

Figure 8. Relative abundance of each form in the cuticle assemblage. Proportions reflect both specimen size and frequency within the assemblage, with the largest segment representing the most dominant form (e.g., Form B) and the smallest segments indicating rare forms. Due to widespread twisting and folding of specimens, proportions are approximate, as precise measurements were challenging. Quantitative data are provided in Table S2.

reported from the upper Shuijingtuo Formation (Cambrian Stage 3) (see fig. 4C in Zhang et al., 2021), although major differences are evident. The Shuijingtuo specimens exhibit pocket mark-type protrusions that are considerably less regular in morphology and significantly larger in individual size compared to the well-defined nodules described here. Similar "ornamented plates" also occur in the Wernecke Mountains of eastern Yukon Territory, northwestern Canada (see figs. 8.11–8.19 in Pyle et al., 2006). Some undetermined specimens (e.g., fig. 8.18 in Pyle et al., 2006) may share the same characteristics as seen in Form E.

Occurrence. Lower part of the Yanjiahe Formation, Muyangxi section, eastern Three Gorges area, Cambrian Fortunian.

Form F

Fig. 6B–D and I–N

Materials. Five specimens.

Description. These cuticular remains bear densely and uniformly distributed short coniform to hook-like spines (Fig. 6B–D and I–N). As for Form E, two subtypes can be distinguished. In subtype 1, spines have a consistent shape (Fig. 6B, C, and I–L), with base widths of 29–51 µm (mean 39.4 µm, $n = 79$) and heights of 36–44 µm (mean 40.4 µm, $n = 7$). Spacing ranges from 39 to 115 µm (mean 64 µm, $n = 60$). All these cuticular elements exhibit wrinkling to varying degrees, with some specimens being intensely crumpled and folded (Fig. 6I–L). Specimen sizes are notably large, with axes measuring 1.92 and 4.32 mm. Some specimens are strongly crumpled (e.g., Fig. 6B), which suggests an original centimetric size. Subtype 2 is characterized by beak-shaped spines (Fig. 6D, M, and N). These spines are arranged in an orderly pattern, with interspinal spacing of 27–69 µm (mean 47.8 µm, $n = 50$) and width of the spine base ranging from 31 to 59 µm (mean 46.6 µm, $n = 29$). The spines are hook-like, resembling a bird's beak, but, unlike the former, their tips are blunt and rounded (Fig. 6M and N). The curved outline of the beak-shaped spines is largely consistent (Fig. 6M and N). No primary features other than spines are observed. The maximal size of this form is about 8.6 mm (Fig. 7; Table S2).

Comparisons. Various Ediacaran to Cambrian organisms possessed spine-like structures especially comparable to subtype 1 (e.g., acanthomorphic acritarchs, *Sterocapsoides wenganensis* in Xiao et al., 2014; and *Mengeosphaera reticulata* in Xiao et al., 2014). However, the pronounced wrinkling and crumpling state of the specimens suggests that this type of cuticle was less rigid than that of Form E. Notably, the spine morphology and distribution pattern show remarkable similarities to *Saccorhytus coronarius* (Han et al., 2017) from the Fortunian Kuanchuanpu Formation, although the spines of *Saccorhytus* are typically more slender. This similarity might suggest a close phylogenetic relationship, potentially placing Form F among basal ecdysozoans. However, the organisms represented by Form F may have been substantially larger (potentially close to centimeter-scale Fig. 7) than *Saccorhytus* (approximately 1 mm), implying that saccorhytids possibly had larger members.

Occurrence. Lower part of the Yanjiahe Formation, Muyangxi section, eastern Three Gorges area, Cambrian Fortunian.

6 Discussion

6.1 Earliest Cambrian ecdysozoan diversity through an "Orsten"-type preservation window

The Ediacaran and Cambrian radiation events mark a key period in animal evolution, witnessing the rapid emergence of fundamental body plans across metazoan lineages (Erwin, 2006). Among these, the Ecdysozoa stand out as both morphologically diverse and ecologically significant (Butterfield, 2003). Critical insights into the early evolution of this clade during the earliest Cambrian come from two key taphonomic windows: "Orsten"-type preservation through early diagenetic phosphatization and small carbonaceous fossil (SCF) assemblages that capture delicate cuticular structures (Maas et al., 2006; Butterfield and Harvey, 2012; Slater et al., 2017, 2018; Slater and Bohlin, 2022; Mussini and Butterfield, 2025). The integrated evidence from "Orsten"-type fossils and SCFs suggest that ecdysozoans diversified during the Fortunian, paralleling the radiation of lophotrochozoans that began in the Terreneuvian (Zhang et al., 2014; Slater and Bohlin, 2022).

The phosphatization process represents a particularly valuable taphonomic pathway (Schiffbauer et al., 2014), with the rapid crystallization of phosphate minerals preserving exceptional soft tissue details ranging from cellular to subcellular levels (Raff et al., 2008; Yin et al., 2014, 2017; Sun et al., 2020, 2021). The fragments in this work display two distinct preservation modes: the secondary permineralized specimens retain original surface relief (e.g., Figs. 2A and 3G–J) and molded counterparts show inverted topographical relationships (e.g., Fig. 2B and D). The first mode corresponds to classic "Orsten"-type preservation, producing phosphatic replicas of cuticular surfaces that appear as crumpled films showing external ornamentation but lacking internal laminar structure or soft tissue information (Maas et al., 2006). The second mode often preserves specimens as impressions within larger phosphatic grains. This preservation type superficially resembles the exuviae of some ecdysozoans (Wang et al., 2019, 2020), as shed cuticles can also display inverted topographic relationships relative to the original surface features. However, the fossils described here differ markedly from exuviae in their substantial thickness (e.g., Fig. 2B and D). We therefore interpret them not as molted cuticles but as molds formed by the impression of the organism's surface onto the surrounding phosphate matrix (e.g., collophanite).

Comparative analysis indicates that our collection contains six potential ecdysozoan taxa. Within these materials, forms C, E, and F (Figs. 4, 5A–C, E, and 6A–D) could potentially belong to sac-like form ecdysozoans, while forms A and D might be attributed to the vermiform organism (Figs. 2, 5D, and 6E, F), with some members possibly bearing limb- (Form A) or setae-like (Form C) structures. More importantly, many specimens exceed 2 mm even in the fragmented state (e.g., Form F; Fig. 7), which suggests that some early

ecdysozoans could attain centimeter sizes. The systematic excavation of additional "Orsten"-type fossils promises to reveal key paleobiological and paleoecological details from macrofaunal specimens.

The early representatives of Ecdysozoa exhibit three fundamental body architectures: an ancestral sac-like form exemplified by Saccorhytida (Han et al., 2017; Liu et al., 2022; Steiner et al., 2020; also see Vannier, 2024, and possibly here forms C, E, and F), a vermiform organization (e.g., *Eopriapulites*; Slater et al., 2018; Slater and Bohlin, 2022; Qin et al., 2023a, b, and possibly here Form D), and panarthropods with limbs or appendage-bearing constructions (Yang et al., 2024; Wang et al., 2025a, and possibly here Form A). Integrated analysis of both body and trace fossils reveals that these distinct forms emerged during the initial phase of the Cambrian explosion (Wang et al., 2025a). The Fortunian fossil record, especially the "Orsten"-type fossils in the Yanjiahe (Fig. 8) and the Kuanchuanpu formations, documents this early diversification (Zhuravlev et al., 2011; Daley et al., 2018; Steiner et al., 2020; Aria, 2022; Kihm et al., 2023; Wang et al., 2025a; this study).

6.2 Morphological affinities and evolutionary significance of Form A: a tentative appendage-bearing Ecdysozoan

Based on the evidence presented here, forms A, B, and D all exhibit lateral branches that vary in size (Figs. 2, 3, and 4D, L). We interpret the branches of Form B as likely representing a form of cuticular spine of the stem-group kinorhynch, rather than true appendages or analogous structures (Fig. 3). In Form D, the branches are notably finer and more delicate, suggesting that they may correspond to setae or similar small cuticular projections of a vermiform animal (Fig. 4L). In contrast, the branches observed in Form A display morphological features more consistent with appendage-like structures, potentially indicating a functional or developmental differentiation from the other forms (Fig. 2). The primary trunk of Form A exhibits broad, although occasionally irregular, transverse annulations on their cuticles. Their consistent width along the body axis in multiple specimens, as opposed to random, post-mortem wrinkles, indicates that these are likely primary anatomical structures, not taphonomic artifacts (Figs. 2 and 6E, F). Similar transverse annulations, although often more pronounced, are characteristic of many Cambrian lobopodians (e.g., *Utahnax vannieri*; Lerosey-Aubril and Ortega-Hernández, 2022). These annulations imply a degree of body flexibility, yet their relatively shallow depth in Form A may suggest a body wall with constrained pliability compared to some lobopodians. This could be an adaptation for increased structural integrity, possibly related to a hydraulic skeleton or serving a protective function in the absence of dorsal spines or sclerites.

Further cuticular detail is provided by a network of finer, elongated, sometimes bifurcating or anastomosing striations (Fig. 2G, H, and K). Comparable micro-ornamentation is known in some lobopodians and early arthropods (Zhang et al., 2007, 2021), potentially representing an integumentary adaptation to balance the mechanical demands of a pressurized hydrostatic skeleton with the flexibility required for locomotion.

The most significant and diagnostic structures are the paired, lateral tubular projections (Fig. 2A, B, I, J, and L). Their general form is reminiscent of the lobopodous appendages of onychophorans and stem-group arthropods (Maas et al., 2007; Zhang et al., 2016). However, critical differences are noted. The appendages of Form A lack the transverse annulations and terminal claws typical of many walking lobopods (Lerosey-Aubril and Ortega-Hernández, 2022). More importantly, their apparent lateral, rather than ventrolateral, insertion on the trunk is a distinctive feature. This lateral insertion argues against a primary function in substrate-based, weight-bearing locomotion (Yang et al., 2024). Instead, it suggests a role in paddling or sediment manipulation, possibly indicative of a crawler rather than walker lifestyle (Maas et al., 2007; Lerosey-Aubril and Ortega-Hernández, 2022; Yang et al., 2024). This morphology distinguishes them from the ventrally located, biramous parapodia of annelids and the dorsoventral body flaps of radiodonts and some lobopodians (Maas et al., 2007; Lerosey-Aubril and Ortega-Hernández, 2022). A superficial resemblance exists to the sensory setae, tractable spines, tubules, or dermal papillae of palaeoscolecidan worms or lobopodians (Maas et al., 2007; Zhang, 2022; Xian et al., 2024a), but the structures in Form A are proportionally much larger and arranged in a distinct, paired serial pattern (Fig. 2A and B).

In summary, Form A is characterized by a cylindrical, annulated, vermiform body bearing serial pairs of lateral, tubular, and likely soft-bodied appendages. Although the fragmentary nature of these specimens limits definitive taxonomic placement, their morphology presents a compelling suite of characters that invite comparison with early ecdysozoans, particularly stem-group panarthropods. If this interpretation is correct, these fossils would represent some of the earliest direct body fossil evidence of appendages in total-group Ecdysozoa, with a Fortunian age aligning temporally with early Cambrian trace fossils (e.g., *Rusophycus avalonensis*, *Monomorphichnus*, and *Allocotichnus dyeri*) potentially attributed to appendage-bearing animals (Zhu, 1997; Weber et al., 2013; Gougeon et al., 2025; Zhang et al., 2025b). While alternative trace-makers (e.g., annelids) for these ichnofossils cannot be ruled out, the co-occurrence of these traces with the fossils with appendages suggests a Fortunian expansion of motile, appendage-bearing bilaterians (Yang et al., 2024; Xian et al., 2026). Current consensus posits that the panarthropod phyla (Euarthropoda, Tardigrada, Onychophora) evolved from a paraphyletic assemblage of soft-bodied, lobopodian-grade organisms bear-

ing appendages (Zhang et al., 2011). The key evolutionary transition from an annulated, soft-bodied lobopodian bauplan toward the fully segmented, sclerotized, and articulated body of crown-group euarthropods fundamentally involved the modification of soft, annulated lobopods into jointed, sclerotized appendages. However, the deeper phylogenetic origins of lobopodians themselves, specifically their derivation from a priapulid-like common ancestor in the ecdysozoan tree, remain a major unresolved question (Budd, 1996; Ortega-Hernández, 2016; Daley et al., 2018). The fossils documented here as Form A may offer valuable insights into this earlier phase of ecdysozoan evolution. Their unique morphological combination of an annulated trunk paired with lateral, non-annulated appendages could represent a primitive grade within lobopodians, a distinct early-diverging ecdysozoan lineage, or even a stem-group priapulid exhibiting unusual lateral structures. Given the fragmentary nature of the material, a definitive taxonomic assignment cannot be established with certainty. Nevertheless, Form A contributes a novel and puzzling data point to our understanding of early panarthropod and ecdysozoan morphological disparity. It reinforces the notion that the Fortunian witnessed not just the first appearance of biomineralized skeletons but also a crucial period of innovation in soft-bodied anatomy, including the early evolution of appendages (Lerosey-Aubril and Ortega-Hernández, 2022).

7 Conclusions

The "Orsten"-type fossils from the early Cambrian provide crucial evidence for the rapid diversification of ecdysozoans during the Fortunian. Our study identifies six forms representing at least four distinct ecdysozoan taxa, including potential scalidophorans and sac-like organisms, with some specimens exceeding 2 mm in size, indicating that early ecdysozoans had already attained large body scales. The widespread development of spines and sclerites across these lineages underscores their adaptive importance, likely serving not only for protection but also for anchoring and other ecological functions. Of particular significance is Form A, which exhibits trunk annulations and paired lateral appendages, suggesting a lobopodian-grade body plan and highlighting early morphological experimentation. Ultimately, ecological expansion appears to have been driven by key innovations such as the evolution of locomotory appendages in panarthropods. Collectively, evidence from "Orsten"-type fossils and small carbonaceous fossils (SCFs) illustrates a dynamic and multifaceted ecdysozoan radiation during the earliest Cambrian, reinforcing the complexity and tempo of early metazoan evolution.

Data availability. Data generated in this study are available in the Supplement.

Supplement. The supplement related to this article is available online at https://doi.org/10.5194/jm-45-455-2026-supplement.

Author contributions. LZ: conceptualization, resources, methodology, investigation, data curation, visualization, validation, and writing (original draft, review, and editing). FZ and YW: data curation, validation, visualization, and writing (review and editing). SC, YYe, YP, LH, QF, MBF, TD, JV, and YYo: writing (original draft, review, and editing). XL: conceptualization, funding acquisition, and writing (review and editing).

Competing interests. At least one of the (co-)authors is a member of the editorial board of *Journal of Micropalaeontology*. The peer-review process was guided by an independent editor, and the authors also have no other competing interests to declare.

Disclaimer. Publisher's note: Copernicus Publications remains neutral with regard to jurisdictional claims made in the text, published maps, institutional affiliations, or any other geographical representation in this paper. The authors bear the ultimate responsibility for providing appropriate place names. Views expressed in the text are those of the authors and do not necessarily reflect the views of the publisher.

Acknowledgements. This work was supported by the National Key Research and Development Program of the Ministry of Science and Technology of China (grant no. 2021YFA0718100), the National Natural Science Foundation of China (grants nos. 41972024 and 41430101), and the Open Foundation of Key Laboratory of Sedimentary Basin and Oil and Gas Resources, Ministry of Natural Resources of China (grant no. cdcgs202200). We sincerely appreciate the assistance provided by Hong-Bing Wang during fieldwork and You-Quan Zhang for his support in sample preparation. We gratefully acknowledge Mingshi Feng for his invaluable support in conducting scanning electron microscopy (SEM) analyses. We extend our sincere thanks to Jingwen Luo and Xianzhi Huang for their invaluable support in figure preparation. We also thank the anonymous reviewer and Shixue Hu for their thorough and constructive critiques, which significantly improved the quality of this work.

Financial support. This research has been supported by the National Natural Science Foundation of China (grant nos. 41972024 and 41430101).

Review statement. This paper was edited by Luke Mander and reviewed by Shixue Hu and one anonymous referee.

References

Aguinaldo, A. M., Turbeville, J. M., Linford, L. S., Rivera, M. C., Garey, J. R., Raff, R. A., and Lake, J. A.: Evidence for a clade of nematodes, arthropods and other moulting animals, Nature, 387, 489–493, https://doi.org/10.1038/387489a0, 1997.

Ahn, S. Y. and Zhu, M. Y.: Lowermost Cambrian acritarchs from the Yanjiahe Formation, South China: Implication for defining the base of the Cambrian in the Yangtze Platform, Geol. Mag., 154, 1217–1231, https://doi.org/10.1017/S0016756816001369, 2017.

Aria, C.: The origin and early evolution of arthropods, Biol. Rev., 97, 1786–1809, https://doi.org/10.1111/brv.12864, 2022.

Bottjer, D. J., Hagadorn, J. W., and Dornbos, S. Q.: The Cambrian substrate revolution, GSA Today, 10, 1–7, 2000.

Brusca, R. C., Moore, W., and Shuster, S. M.: Invertebrates, in: 3rd Edn. Sinauer Associates Inc, Publishers, Sunderland, MA, 1104 pp., ISBN 9781605353753, 2016.

Budd, G. E.: The morphology of *Opabinia regalis* and the reconstruction of the arthropod stem-group, Lethaia, 29, 1–14, https://doi.org/10.1111/j.1502-3931.1996.tb01831.x, 1996.

Butterfield, N. J.: Exceptional fossil preservation and the Cambrian explosion, Integrat. Comparat. Biol., 43, 166–177, https://doi.org/10.1093/icb/43.1.166, 2003.

Butterfield, N. J. and Harvey, T. H. P.: Small carbonaceous fossils (SCFs): A new measure of early Paleozoic paleobiology, Geology, 40, 71–74, https://doi.org/10.1130/G32580.1, 2012.

Carlisle, E., Yin, Z. J., Pisani, D., and Donoghue, P. C.: Ediacaran origin and Ediacaran-Cambrian diversification of Metazoa, Sci. Adv., 10, eadp7161, https://doi.org/10.1126/sciadv.adp7161, 2024.

Chang, S., Zhang, L., Clausen, S., Bottjer, D. J., and Feng, Q. L.: The Ediacaran-Cambrian rise of siliceous sponges and development of modern oceanic ecosystems, Precamb. Res., 333, 105438, https://doi.org/10.1016/j.precamres.2019.105438, 2019.

Chen, P.: Discovery of lower Cambrian small shelly fossils from Jijiapo, Yichang, West Hubei and its significance, Profess. Pap. Stratigr. Palaeontol., 13, 49–64, 1984.

Chen, Q., Sun, M., Long, X. P., Zhao, G. C., Wang, J., Yu, Y., and Yuan, C.: Provenance study for the Paleozoic sedimentary rocks from the west Yangtze Block: constraint on possible link of South China to the Gondwana supercontinent reconstruction, Precamb. Res., 309, 271-289, https://doi.org/10.1016/j.precamres.2017.01.022, 2018a.

Chen, Z. and Liu, Y. R.: Advent of three-dimensional sediment exploration reveals Ediacaran-Cambrian ecosystem transition, Sci. Adv., 11, eadx9449, https://doi.org/10.1126/sciadv.adx9449, 2025.

Chen, Z., Chen, X., Zhou, C. M., Yuan, X. L., and Xiao, S. H.: Late Ediacaran trackways produced by bilaterian animals with paired appendages, Sci. Adv., 4, eaao6691, https://doi.org/10.1126/sciadv.aao6691, 2018b.

Chen, Z., Zhou, C. M., Yuan, X. L., and Xiao, S. H.: Death march of a segmented and trilobate bilaterian elucidates early animal evolution, Nature, 573, 412–415, https://doi.org/10.1038/s41586-019-1522-7, 2019.

Condon, D., Zhu, M. Y., Bowring, S., Wang, W., Yang, A. H., and Jin, Y. G.: U-Pb ages from the Neoproterozoic Doushantuo Formation, China, Science, 308, 95–98, https://doi.org/10.1126/science.1107765, 2005.

Crimes, T. P. and Anderson, M. M.: Trace fossils from Late Precambrian–Early Cambrian strata of Southeastern Newfoundland (Canada): Temporal and environmental implications, J. Paleontol., 59, 310–343, 1985.

Daley, A. C., Antcliffe, J. B., Drage, H. B., and Pates, S.: Early fossil record of Euarthropoda and the Cambrian Explosion, P. Natl. Acad. Sci. USA, 115, 5323–5331, https://doi.org/10.1073/pnas.1719962115, 2018.

Dong, X. P., Donoghue, P. C., Cheng, H., and Liu, J. B.: Fossil embryos from the Middle and Late Cambrian period of Hunan, South China, Nature, 427, 237–240, https://doi.org/10.1038/nature02215, 2004.

Dong, X. P., Bengtson, S., Gostling, N. J., Cunningham, J. A., Harvey, T. H., Kouchinsky, A., Val'Kov, A. K., Repetski, J. E., Stampanoni, M., Marone, F., and Donoghue, P. C.: The anatomy, taphonomy, taxonomy and systematic affinity of *Markuelia*: Early Cambrian to Early Ordovician scalidophorans, Palaeontology, 53, 1291–1314, https://doi.org/10.1111/j.1475-4983.2010.01006.x, 2010.

Edgecombe, G. D.: Arthropod origins: Integrating paleontological and molecular evidence, Annu. Rev. Ecol. Evol. Syst., 51, 1–25, https://doi.org/10.1146/annurev-ecolsys-011720-124437, 2020.

Edgecombe, G. D. and Legg, D. A.: Origins and early evolution of arthropods, Palaeontology, 57, 457–468, https://doi.org/10.1111/PALA.12105, 2014.

Erwin, D. H.: The developmental origins of animal bodyplans. *In:* Xiao, S. H., and Kaufman, A. J., Ed, Neoproterozoic Geobiology and Paleobiology, Springer Netherlands, Dordrecht, 159–197, https://doi.org/10.1007/1-4020-5202-2_6, 2006.

Erwin, D. H., Laflamme, M., Tweedt, S. M., Sperling, E. A., Pisani, D., and Peterson, K. J.: The Cambrian conundrum: early divergence and later ecological success in the early history of animals, Science, 334, 1901–1907, https://doi.org/10.1126/science.1206375, 2011.

Gao, P., Li, S. J., Lash, G. G., Yan, D. T., Zhou, Q., and Xiao, X. M.: Stratigraphic framework, redox history, and organic matter accumulation of an Early Cambrian intra platform basin on the Yangtze Platform, South China, Mar. Petrol. Geol., 130, 105095, https://doi.org/10.1016/j.marpetgeo.2021.105095, 2021.

Giribet, G. and Edgecombe, G. D.: Current understanding of Ecdysozoa and its internal phylogenetic relationships, Integrat. Comparat. Biol., 57, 455–466, https://doi.org/10.1093/icb/icx072, 2017.

Gougeon, R., Mángano, M. G., Buatois, L. A., Narbonne, G. M., Laing, B. A., and Paz, M.: Ichnology of the Ediacaran–Cambrian Chapel Island Formation of Newfoundland, Canada: unraveling bioturbation at the onset of the Cambrian Explosion, Fossils Strata, 72, 1–214, https://doi.org/10.18261/9788294167128-2025-01, 2025.

Guo, J. F., Li, Y., Han, J., Zhang, X. L., Zhang, Z. F., Ou, Q., and Shu, D. G.: Discovery of Genus Protoconites Chen et al., 1994 from Yanjiahe Formation, Terreneuvian of the Three Gorge area, South China, Prog. Nat. Sci., 19, 180–184, https://doi.org/10.3321/j.issn:1002-008X.2009.02.008, 2009.

Guo, J. F., Li, Y., and Li, G. X.: Small shelly fossils from the early Cambrian Yanjiahe Formation, Yichang, Hubei, China, Gondwana Res., 25, 999–1007, https://doi.org/10.1016/j.gr.2013.03.007, 2014.

Guo, J. F., Han, J., Iten, H. V., Wang, X., Qiang, Y. Q., Song, Z. C., Wang, W. Z., Zhang, Z. F., and Li, G. X.: A fourteen-faced hexangulaconulariid from the early Cambrian (Stage 2) Yanjiahe Formation, South China, J. Paleontol., 94, 45–55, https://doi.org/10.1017/jpa.2019.56, 2020.

Han, J., Morris, S. C., Ou, Q., Shu, D. G., and Huang, H.: Meiofaunal deuterostomes from the basal Cambrian of Shaanxi (China), Nature, 542, 228–231, https://doi.org/10.1038/nature21072, 2017.

Haug, J. T., Maas, A., Waloszek, D., Donoghue, P. C., and Bengtson, S.: A new species of '*Markuelia*' from the Middle Cambrian of Australia, Memoir. Assoc. Austral. Palaeontol., 37, 303–313, 2009.

Howard, R. J., Giacomelli, M., Lozano-Fernandez, J., Edgecombe, G. D., Fleming, J. F., Kristensen, R. M., Ma, X., Olesen, J., Sørensen, M. V., Thomsen, P. F., Wills, M. A., Donoghue, P. C. J., and Pisani, D.: The Ediacaran origin of Ecdysozoa: Integrating fossil and phylogenomic data, J. Geol. Soc., 179, jgs202-107, https://doi.org/10.1144/jgs2021-107, 2022.

Hughes, I. V., Evans, S. D., and Droser, M. L.: An Ediacaran bilaterian with an ecdysozoan affinity from South Australia, Curr. Biol., 34, 5782–5788, https://doi.org/10.1016/j.cub.2024.10.030, 2024.

Ishikawa, T., Ueno, Y., Komiya, T., Sawaki, Y., Han, J., Shu, D. G., Li, Y., Maruyama, S., and Yoshida, N.: Carbon isotope chemostratigraphy of a Precambrian/Cambrian boundary section in the Three Gorge area, South China: Prominent global-scale isotope excursions just before the Cambrian Explosion, Gondwana Res., 14, 193–208, https://doi.org/10.1016/j.gr.2007.10.008, 2008.

Kapli, P., Flouri, T., and Telford, M. J.: Systematic errors in phylogenetic trees, Curr. Biol., 31, R59–R64, https://doi.org/10.1016/j.cub.2020.11.043, 2021.

Kihm, J. H., Smith, F. W., Kim, S., Rho, H. S., Zhang, X., Liu, J., and Park, T. Y. S.: Cambrian lobopodians shed light on the origin of the tardigrade body plan, P. Natl. Acad. Sci. USA 120, e2211251120, https://doi.org/10.1073/pnas.2211251120, 2023.

Lan, Z. W., Li, X. H., Chu, X. L., Tang, G. Q., Yang, S. H., Yang, H. W., Liu, H., Jiang, T., and Wang, T.: SIMS U-Pb zircon ages and Ni-Mo-PGE geochemistry of the lower Cambrian Niutitang Formation in South China: Constraints on Ni-Mo-PGE mineralization and stratigraphic correlations, J. Asian Earth Sci., 137, 141–162, https://doi.org/10.1016/j.jseaes.2016.12.046, 2017.

Lee, M. S., Jago, J. B., García-Bellido, D. C., Edgecombe, G. D., Gehling, J. G., and Paterson, J. R.: Modern optics in exceptionally preserved eyes of Early Cambrian arthropods from Australia, Nature, 474, 631–634, https://doi.org/10.1038/nature10097, 2011.

Lerosey-Aubril, R. and Ortega-Hernández, J.: A new lobopodian from the middle Cambrian of Utah: did swimming body flaps convergently evolve in stem-group arthropods?, Pap. Palaeontol., 8, e1450, https://doi.org/10.1002/spp2.1450, 2022.

Linnemann, U., Ovtcharova, M., Schaltegger, U., Gärtner, A., Hautmann, M., Geyer, G., Vickers-Rich, P., Rich, T., Plessen, B., Hofmann, M., Zieger, J., Krause, R., Kriesfeld, L., and Smith, J.: New high-resolution age data from the Ediacaran–Cambrian boundary indicate rapid, ecologically driven onset of the Cambrian explosion, Terra Nova, 31, 49–58, https://doi.org/10.1111/ter.12368, 2019.

Liu, A. G.: Evolution: An Ediacaran ecdysozoan, Curr. Biol., 35, R26–R28, https://doi.org/10.1016/j.cub.2024.11.030, 2025.

Liu, M. J., Xian, X. F., Zhang, H. Q., Eriksson, M. E., Liu, Y. H., and and Shao, T. Q.: New ecdysozoan fossil embryos from the basal Cambrian of China, Palaeogeogr. Palaeocl. Palaeoecol., 659, 112635, https://doi.org/10.1016/j.palaeo.2024.112635, 2025.

Liu, Y. H., Li, Y., Shao, T. Q., Zhang, H. Q., Wang, Q. and Qiao, J. P.: *Quadrapyrgites* from the lower Cambrian of South China: Growth pattern, post-embryonic development, and affinity, Chinese Sci. Bull., 59, 4086–4095, https://doi.org/10.1007/s11434-014-0481-5, 2014.

Liu, Y. H., Qin, J, C., Wang, Q., Maas, A., Duan, B. C., Zhang, Y. N., Zhang, H., Shao, T. Q., and Zhang, H. Q.: New armoured scalidophorans (Ecdysozoa, Cycloneuralia) from the Cambrian Fortunian Zhangjiagou Lagerstätte, South China, Pap. Palaeontol., 5, 241–260, https://doi.org/10.1002/spp2.1239, 2018.

Liu, Y. H., Carlisle, E., Zhang, H. Q., Yang, B., Steiner, M., Shao, T. Q., Duan, B. C., Marone, F., Xiao, S. H., and Donoghue, P. C.: *Saccorhytus* is an early ecdysozoan and not the earliest deuterostome, Nature, 609, 541–546, https://doi.org/10.1038/s41586-022-05107-z, 2022.

Luzhnaya, E. A., Zhegallo, E. A., Zaitseva, L. V., and Ragozina, A. L.: Problematical Porifera from the Lower Cambrian of Western Mongolia, Paleontol. J., 57, 256–269, https://doi.org/10.31857/S0031031X2303011X, 2023.

Maas, A., Braun, A., Dong, X. P., Donoghue, P. C., Müller, K. J., Olempska, E., Repetski, J. E., Siveter, D. J., Stein, M., and Waloszek, D.: The 'Orsten' – More than a Cambrian Konservat-Lagerstätte yielding exceptional preservation, Palaeoworld, 15, 266–282, https://doi.org/10.1016/j.palwor.2006.10.005, 2006.

Maas, A., Mayer, G., Kristensen, R. M., and Waloszek, D.: A Cambrian micro-lobopodian and the evolution of arthropod locomotion and reproduction, Chinese Sci. Bull., 52, 3385–3392, https://doi.org/10.1007/s11434-007-0515-3, 2007.

Mángano, M. G. and Buatois, L. A.: Decoupling of body-plan diversification and ecological structuring during the Ediacaran–Cambrian transition: Evolutionary and geobiological feedbacks, P. Roy. Soc. B, 281, 20140038, https://doi.org/10.1098/rspb.2014.0038, 2014.

Metcalfe, I.: Gondwana dispersion and Asian accretion: Tectonic and palaeogeographic evolution of eastern Tethys, J. Asian Earth Sci., 66, 1–33, https://doi.org/10.1016/j.jseaes.2012.12.020, 2013.

Mussini, G. and Butterfield, N. J.: Exotic cuticular specializations in a Cambrian scalidophoran, P. Roy. Soc. B, 292, 20242806, https://doi.org/10.1098/rspb.2024.2806, 2025.

Nielsen, C.: Animal Evolution: Interrelationships of the Living Phyla, in: 3rd Edn., Oxford University Press, Oxford, 1–389, https://doi.org/10.1093/acprof:oso/9780199606023.001.0001, 2012.

Okada, Y., Sawaki, Y., Komiya, T., Hirata, T., Takahata, N., Sano, Y., Maruyama, S., and Maruyama, S.: New chronological constraints for Cryogenian to Cambrian rocks in the Three Gorges, Weng'an and Chengjiang areas, South China, Gondwana Res., 25, 1027–1044, https://doi.org/10.1016/j.gr.2013.05.001, 2014.

Ortega-Hernández, J.: Making sense of 'lower' and 'upper' stem–group Euarthropoda, with comments on the strict use of the name Arthropoda von Siebold, 1848, Biol. Rev., 91, 255–273, https://doi.org/10.1111/brv.12168, 2016.

Paterson, J. R., García-Bellido, D. C., Lee, M. S., Brock, G. A., Jago, J. B., and Edgecombe, G. D.: Acute vision in the giant Cambrian predator Anomalocaris and the origin of compound eyes, Nature, 480, 237–240, https://doi.org/10.1038/nature10689, 2011.

Peng, S. C., Babcock, L. E., and Cooper, R. A.: The Cambrian Period, in: The Geologic Time Scale 2012, edited by: Gradstein, F. M., Ogg, J. G., Schmitz, M. D., and Ogg, G. M., Elsevier BV, Amsterdam, 437–488, ISBN 978-0-444-59425-9, 2012.

Pyle, L. J., Narbonne, G. M., Nowlan, G. S., Xiao, S., and James, N. P.: Early Cambrian metazoan eggs, embryos, and phosphatic microfossils from northwestern Canada, J. Paleontol., 80, 811–825, https://doi.org/10.1666/0022-3360(2006)80[811:ECMEEA]2.0.CO;2, 2006.

Qian, Y.: Hyolitha and some problematica from the Lower Cambrian Meishucunian Stage in central and southwestern China, Acta Palaeontol. Sin., 16, 255–275, 1977.

Qin, J. C., Liu, Y. H., Shao, T. Q., Liu, M. J., and Zhang, Y. N.: Growth pattern of Fortunian scalidophoran sclerites, Front. Earth Sci., 11, 1210062, https://doi.org/10.3389/feart.2023.1210062, 2023a.

Qin, J. C., Liu, Y. H., Shao, T. Q., Wang, Q., Zhang, Y. N., Zhou, X. Y., and Liu, M. J.: Three indeterminate forms of scalidophoran worms from the Cambrian Fortunian of South China, Acta Geol. Sin., 97, 1026–1037, https://doi.org/10.1111/1755-6724.15052, 2023b.

Raff, E. C., Schollaert, K. L., Nelson, D. E., Donoghue, P. C. J., Thomas, C. W., Turner, F. R., Stein, B. D., Dong, X. P., Bengtson, S., Huldtgren, T., Stampanoni, M., Yin, C. Y., and Raff, R. A.: Embryo fossilization is a biological process mediated by microbial biofilms, P. Natl. Acad. Sci. USA, 105, 19360–19365, https://doi.org/10.1073/pnas.0810106105, 2008.

Rota-Stabelli, O., Daley, A. C., and Pisani, D.: Molecular timetrees reveal a Cambrian colonization of land and a new scenario for ecdysozoan evolution, Curr. Biol., 23, 392–398, https://doi.org/10.1016/j.cub.2013.01.026, 2013.

Schiffbauer, J. D., Wallace, A. F., Broce, J., and Xiao, S. H.: Exceptional fossil conservation through phosphatization, Paleontol. Soc. Pap., 20, 59–82, https://doi.org/10.1017/S1089332600002801, 2014.

Seilacher, A.: Spuren und fazies im Unterkambrium, in: Beiträge zur Kenntnis des Kambriums in der Salt Range (Pakistan), edited by: Schindewolf, O. and Seilacher, A., Akademie der Wissenschaften under Literatur, Mainz, Abhandlungen der mathematisch-naturwissenschaftlichen Klasse, 10, 261–446, 1955.

Shao, T. Q., Qin, J. C., Shao, Y., Liu, Y. H., Waloszek, D., Maas, A., Duan, B. C., Wang, Q., Xu, Y., and Zhang, H. Q.: New macrobenthic cycloneuralians from the Fortunian (lowermost Cambrian) of South China, Precamb. Res., 349, 105413, https://doi.org/10.1016/j.precamres.2019.105413, 2020a.

Shao, T. Q., Wang, Q., Liu, Y. H., Qin, J. C., Zhang, Y. N., Liu, M. J., Shao, Y., Zhao, J. Y., and Zhang, H. Q.: A new scalidophoran animal from the Cambrian Fortunian Stage of South China and its implications for the origin and early evolution of Kinorhyncha, Precamb. Res., 349, 105616, https://doi.org/10.1016/j.precamres.2020.105616, 2020b.

Slater, B. J. and Bohlin, M. S.: Animal origins: The record from organic microfossils, Earth-Sci. Rev., 232, 104107, https://doi.org/10.1016/j.earscirev.2022.104107, 2022.

Slater, B. J., Harvey, T. H., Guilbaud, R., and Butterfield, N. J.: A cryptic record of Burgess Shale-type diversity from the early Cambrian of Baltica, Palaeontology, 60, 117–140, https://doi.org/10.1111/pala.12273, 2017.

Slater, B. J., Harvey, T. H. P., and Butterfield, N. J.: Small carbonaceous fossils (SCFs) from the Terreneuvian (lower Cambrian) of Baltica, Palaeontology, 61, 417–439, https://doi.org/10.1111/pala.12350, 2018.

Song, Z. C., Guo, J. F., Han, J., Van Iten, H., Peng, J. X., Qiang, Y. Q., Zhang, B. Y., Zhao, X. F., Li, G. X., and Wen, H. J.: Phylogenetic affinities and evolution of the Early Cambrian hexangulaconulariids, J. Syst. Palaeontol., 22, 2417668, https://doi.org/10.1080/14772019.2024.2417668, 2024.

Steiner, M., Li, G. X., Qian, Y., Zhu, M. Y., and Erdtmann, B.-D.: Neoproterozoic to Early Cambrian small shelly fossil assemblages and a revised biostratigraphic correlation of the Yangtze Platform (China), Palaeogeogr. Palaeocl. Palaeoecol., 254, 67–99,https://doi.org/10.1016/j.palaeo.2007.03.046, 2007.

Steiner, M., Yang, B., Hohl, S., Zhang, L., and Chang, S.: Cambrian small skeletal fossil and carbon isotope records of the southern Huangling Anticline, Hubei (China) and implications for chemostratigraphy of the Yangtze Platform, Palaeogeogr. Palaeocl. Palaeoecol., 554, 109817, https://doi.org/10.1016/j.palaeo.2020.109817, 2020.

Sun, W. C., Yin, Z. J., Cunningham, J. A., Liu, P. J., Zhu, M. Y., and Donoghue, P. C. J.: Nucleus preservation in early Ediacaran Weng'an embryo-like fossils, experimental taphonomy of nuclei and implications for reading the eukaryote fossil record, Interface Focus, 10, 20200015, https://doi.org/10.1098/rsfs.2020.0015, 2020.

Sun, W. C., Yin, Z. J., Liu, P. J., Donoghue, P. C. J., Li, J. H., and Zhu, M. Y.: Ultrastructure and in-situ chemical characterization of intracellular granules of embryo-like fossils from the early Ediacaran Weng'an Biota, PalZ, 95, 611–621, https://doi.org/10.1007/s12542-021-00597-0, 2021.

Vannier, J.: The early Cambrian *Saccorhytus* is a non-feeding larva of a scalidophoran worm, P. Roy. Soc. B, 291, 20241256, https://doi.org/10.1098/rspb.2024.1256, 2024.

Vannier, J., Steiner, M., Renvoisé, E., Hu, S. X., and Casanova, J. P.: Early Cambrian origin of modern food webs: Evidence from predator arrow worms, P. Roy. Soc. B, 274, 627–633, https://doi.org/10.1098/rspb.2006.3761, 2007.

Vannier, J., Calandra, I., Gaillard, C., and Żylińska, A.: Priapulid worms: Pioneer horizontal burrowers at the Precambrian-Cambrian boundary, Geology, 38, 711–714, https://doi.org/10.1130/G30829.1, 2010.

Wang, D., Ling, H. F., Li, D., and Chen, X.: Carbon isotope stratigraphy of Yanjiahe Formation across the Ediacaran–Cambrian boundary in the area of the Three Gorges, J. Stratigr., 36, 21–30, 2012.

Wang, D., Vannier, J., Schumann, I., Wang, X., Yang, X. G., Komiya, T., Uesugi, K., Sun, J., and Han, J.: Origin of ecdysis: fossil evidence from 535-million-year-old scalidophoran worms, P. Roy. Soc. B, 286, 20190791, https://doi.org/10.1098/rspb.2019.0791, 2019.

Wang, D., Vannier, J., Yang, X. G., Sun, J., Sun, Y. F., Hao, W. J., Tang, Q. Q., Liu, P., and Han, J.: Cuticular reticulation replicates the pattern of epidermal cells in lowermost Cambrian scalidophoran worms, P. Roy. Soc. B, 287, 20200470, https://doi.org/10.1098/rspb.2020.0470, 2020.

Wang, D., Vannier, J., Sun, J., Yu, C. Y., and Han, J.: A new Chengjiang worm sheds light on the radiation and disparity in early Priapulida, Biology, 12, 1242, https://doi.org/10.3390/biology12091242, 2023a.

Wang, D., Qiang, Y. Q., Guo, J. F., Vannier, J., Song, Z. C., Peng, J. X., Zhang, B. Y., Sun, J., Yu, Y. L., Zhang, Y. H., Zhang, T., Yang, X. G., and Han, J.: Early evolution of the ecdysozoan body plan, eLife, 13, RP94709, https://doi.org/10.7554/eLife.94709.3, 2024.

Wang, D., Han, J., Guo, J. F., and Qiang, Y. Q.: Origin and evolution of bodyplans of ecdysozoans during the Cambrian explosion, Chin. J. Nature, 47, 125–133, https://doi.org/10.3969/j.issn.0253-9608.2025.02.004, 2025a.

Wang, D., Vannier, J., Martín-Durán, J. M., Herranz, M., and Yu, C. Y.: Preservation and early evolution of scalidophoran ventral nerve cord, Sci. Adv., 11, eadr0896, https://doi.org/10.1126/sciadv.adr0896, 2025b.

Wang, J. and Li, Z. X.: History of Neoproterozoic rift basins in South China: implications for Rodinia break-up, Precamb. Res., 122, 141–158, https://doi.org/10.1016/S0301-9268(02)00209-7, 2003.

Wang, L. J., Lin, S. F., and Xiao, W. J.: Yangtze and Cathaysia blocks of South China: Their separate positions in Gondwana until early Paleozoic juxtaposition, Geology, 51, 723–727, https://doi.org/10.1130/G51362.1, 2023b.

Wang, X. F., Erdtmann, B. D., Chen, X. H., and Mao, X. D.: Integrated sequence-, bio-and chemostratigraphy of the terminal Proterozoic to Lowermost Cambrian "black rock series" from central South China, Episodes J. Int. Geosci., 21, 178–189, https://doi.org/10.18814/epiiugs/1998/v21i3/007, 1998.

Weber, B., Steiner, M., Evseev, S., and Yergaliev, G.: First report of a Meishucun-type early Cambrian (Stage 2) ichnofauna from the Malyi Karatau area (SE Kazakhstan), Palaeoichnological, palaeoecological and palaeogeographical implications, Palaeogeogr. Palaeocl. Palaeoecol., 392, 209–231, https://doi.org/10.1016/j.palaeo.2013.08.021, 2013.

Xian, X. F., Eriksson, M. E. and Zhang, H. Q.: Growth patterns of palaeoscolecid sclerites from the Furongian (upper Cambrian) Wangcun section, western Hunan, South China, Palaeoworld, 33, 284–298, https://doi.org/10.1016/j.palwor.2023.03.005, 2024a.

Xian, X. F., Eriksson, M. E., and Zhang, H. Q.: Reassessment of *Archaeooides* based on new material from the Fortunian (early Cambrian) of China infers algal affinity, Palaeogeogr. Palaeocl. Palaeoecol., 637, 112011, https://doi.org/10.1016/j.palaeo.2023.112011, 2024b.

Xian, X. F., Zhang, H. Q., Xiao, S. H., Waloszek, D., Maas, A., and Duan, B. C.: Polychaete annelids from the earliest Cambrian Period, P. Natl. Acad. Sci. USA, 123, e2538071123, https://doi.org/10.1073/pnas.2538071123, 2026.

Xiao, S. H., Zhou, C. M., Liu, P. J., Wang, D., and Yuan, X. L.: Phosphatized acanthomorphic acritarchs and related microfossils from the Ediacaran Doushantuo Formation at Weng'an (South China) and their implications for biostratigraphic correlation, J. Paleontol., 88, 1–67, https://doi.org/10.1666/12-157R, 2014.

Yang, X., Wang, D., Zhang, Z. L., Wang, X., Sun, J., Hao, W. J., Liu, Y. Q., Uesugi, K., Komiya, T., and Han, J.: Basal Cambrian soft-bodied segmented bilaterians preserved as microbial pseudomorphs, bioRxiv, 2024-07, https://doi.org/10.1101/2024.07.03.601876, 2024.

Yin, Z. J., Liu, P. J., Li, G., Tafforeau, P., and Zhu, M. Y.: Biological and taphonomic implications of Ediacaran fossil embryos undergoing cytokinesis, Gondwana Res., 25, 1019–1026, https://doi.org/10.1016/j.gr.2013.01.008, 2014.

Yin, Z. J., Cunningham, J. A., Vargas, K., Bengtson, S., Zhu, M. Y., and Donoghue, P. C. J.: Nuclei and nucleoli in embryo-like fossils from the Ediacaran Weng'an Biota, Precamb. Res., 301, 145–151, https://doi.org/10.1016/j.precamres.2017.08.009, 2017.

Yu, C.Y., Wang, D., Yong, Y. Y., Tang, Q. Q., Hao, W. J.., Sun, J., Yang, X. G., He, K. Y., Yue, N., and Han, J.: Ecdysis of *Eopriapulites sphinx* from the early Cambrian Kuanchuanpu biota, Acta Micropalaeontol. Sin., 39, 285–291, https://doi.org/10.16087/j.cnki.1000-0674.20221118.001, 2022.

Zhang, H. Q.: The evolutionary relationships of the earliest known cycloneuralians and a new record from the Cambrian Fortunian of South China, Palaeoworld, 31, 389–401, https://doi.org/10.1016/j.palwor.2021.09.003, 2022.

Zhang, H. Q., Xiao, S. H., Liu, Y. H., Yuan, X. L., Wan, B., Muscente, A. D., Shao, T. Q., Gong, H. and Cao, G. H.: Armored kinorhynch-like scalidophoran animals from the early Cambrian, Sci. Rep., 5, 16521, https://doi.org/10.1038/srep16521, 2015.

Zhang, H. Q., Maas, A., and Waloszek, D.: New material of scalidophoran worms in 'Orsten'-type preservation from the Cambrian Fortunian Stage of South China, J. Paleontol., 92, 14–25, https://doi.org/10.1017/jpa.2017.39, 2018.

Zhang, L., Chang, S., Chen, C., Eriksson, M. E., Feng, Q. L., Steiner, M., Khan, M. Z., Vannier, J., Forel, M. B., and Clausen, S.: Diverse cuticular remains in Cambrian (Series 2) SSF assemblages from China and the pioneer metazoan colonization of offshore environments, Palaeogeogr. Palaeocl. Palaeoecol., 567, 110192, https://doi.org/10.1016/j.palaeo.2020.110192, 2021.

Zhang, L., Chang, S., Chen, C., Wang, X., Feng, Q. L., Steiner, M., Yang, B., Mason, R., She, Z. B., Yan, J. X., Vannier, J., Forel, M. B., Xiao, Q., and Clausen, S.: *Cloudina* aggregates from the uppermost Dengying Formation, Three Gorges area, South China, and stratigraphical implications, Precambrian Res., 370, 106552, https://doi.org/10.1016/j.precamres.2021.106552, 2022.

Zhang, L., Wu, Y., Zhai, F., Duan, C. Z., Fu, S. S., Chang, S., Ye, Y., Chen, C., Wang, X., Lang, X. G., Feng, Q. L., and Forel, M. B.: The earliest sponge spicule tufts from the Cambrian Lower Yanjiahe Formation, Three Gorges area, South China, Palaeoworld, 34, 200995, https://doi.org/10.1016/j.palwor.2025.200995, 2025a.

Zhang, L. J., Buatois, L. A., Mángano, M. G., Yang, Q., Zhang, S., Wei, F., Fan, R. Y., Zhao, Z., Wang, Z., Ma, X. Y., and Tang, F.: Trace fossils from the Meishucun section of South China: Revisiting ichnotaxonomy, behavioural diversification and ecosystem engineering from a key Ediacaran–Cambrian succession, Pap. Palaeontol., 11, e70009, https://doi.org/10.1002/spp2.70009, 2025b.

Zhang, X. G.: Moult stages and dimorphism of Early Cambrian bradoriids from Xichuan, Henan, China, Alcheringa, 11, 1–19, https://doi.org/10.1080/03115518708618976, 1987.

Zhang, X. G., Siveter, D. J., Waloszek, D., and Maas, A.: An epipodite-bearing crown-group crustacean from the Lower Cambrian, Nature, 449, 595–598, https://doi.org/10.1038/nature06138, 2007.

Zhang, X. G., Pratt, B. R., and Shen, C.: Embryonic development of a Middle Cambrian (500 myr old) scalidophoran worm, J. Paleontol., 85, 898–903, https://doi.org/10.1666/11-024.1, 2011.

Zhang, X. G., Smith, M. R., Yang, J., and Hou, J. B.: Onychophoran-like musculature in a phosphatized Cambrian lobopodian, Biol. Lett., 12, 20160492, https://doi.org/10.1098/rsbl.2016.0492, 2016.

Zhang, X. L. and Shu, D. G.: Current understanding on the Cambrian Explosion: Questions and answers, PalZ, 95, 641–660, https://doi.org/10.1007/s12542-021-00568-5, 2021.

Zhang, X. L., Shu, D. G., Han, J., Zhang, Z. F., Liu, J. N., and Fu, D. J.: Triggers for the Cambrian explosion: Hypotheses and problems, Gondwana Res., 25, 896–909, https://doi.org/10.1016/j.gr.2013.06.001, 2014.

Zhou, C. M., Brasier, M. D., and Xue, Y. S.: Three-dimensional phosphatic preservation of giant acritarchs from the terminal Proterozoic Doushantuo Formation in Guizhou and Hubei provinces, South China, Palaeontology, 44, 1157–1178, https://doi.org/10.1111/1475-4983.00219, 2001.

Zhu, M. Y.: Precambrian–Cambrian trace fossils from eastern Yunnan: Implications for Cambrian explosion, Bull. Natl. Museum Nat. Sci., 10, 275–312, 1997.

Zhu, M. Y., Zhang, J. M., Steiner, M., Yang, A. H., Li, G. X., and Erdtmann, B.-D.: Sinian-Cambrian stratigraphic framework for shallow-to deep-water environments of the Yangtze Platform: an integrated approach, Prog. Nat. Sci., 13, 951–960, https://doi.org/10.1080/10020070312331344710, 2003.

Zhu, M. Y., Zhang, J. M., and Yang, A. H.: Integrated Ediacaran (Sinian) chronostratigraphy of South China, Palaeogeogr. Palaeocl. Palaeoecol., 254, 7–61, https://doi.org/10.1016/j.palaeo.2007.03.025, 2007.

Zhuravlev, A. Y., Gámez Vintaned, J. A., and Liñán, E.: The Palaeoscolecida and the evolution of the Ecdysozoa, Palaeontogr. Canad., 31, 177–204, 2011.